Phosphodiesterase 10A Upregulation Contributes to Pulmonary Arterial Hypertension

Inaugural Dissertation
submitted to the
Faculty of Medicine
in partial fulfillment of the requirements
for the degree of Doctor of Human Biology
in the Faculty of Medicine
of the Justus Liebig University of Giessen

by
Xia Tian
of
Jiangsu, China

Giessen, 2009

From the Department of Internal Medicine

Director/Chairman: Prof. Dr. med. Werner Seeger
of the University Hospital Giessen - Marburg

Supervisor: Prof. Dr. rer. nat. Ralph Theo Schermuly

Gutachter: Prof. Dr. Ralph Theo Schermuly
Gutachter: Prof. Dr. Gerhild Euler

Date of Doctoral Defense: 12th April 2010

INDEX

LIST OF FIGURES

LIST OF TABLES

ABBREVIATIONS

AC	adenylyl cyclase
APS	ammonium persulfate
ANP	atrial natriuretic peptide
αSMA	alpha smooth muscle actin
BNP	brain natriuretic peptide
bp	base pairs
BSA	bovine serum albumin
cAMP	cyclic 3'5'-adenosine monophosphate
cDNA	complementary deoxyribonucleic acid
cGMP	cyclic 3'5'-guanosine monophosphate
cpm	counts per minute
CREB	cAMP-response element binding protein
Ct	threshold cycle
ΔΔCt	delta-delta Ct
°C	centigrade
Da	dalton
DAPI	4’,6-diamidino-2-phenylindole
DEPC	diethyl-pyrocarbonate
DMEM	dulbecco's modified eagle's medium
DMSO	dimethyl sulfoxide
dNTP	deoxyribonucleotide triphosphate
DTT	dithiothreitol
EDTA	ethylendinitrilo-N,N,N’,N’ tetra acetate
EHNA	erythro-9-(2-Hydroxy-3-nonyl)adenine
eNOS	endothelial nitric oxide synthase
et al.	*et alii* (and others)
ET-1	endothelin-1
ETA	endothelin receptor A
ETB	endothelin receptor B
FBS	fetal bovine serum
FITC	fluorescein-5-isothiocyanate
g	gram

GAPDH	glyceraldehyde 3-phosphate dehydrogenase
h	hour(s)
HBSS	hanks' balanced salt solution
HEPES	4-(2-hydroxyethyl)-1-piperazineethanesulfonic acid
5-HT	5-hydroxy tryptamine
5-HTT	5-hydroxy tryptamine transporter
IPAH	idiopathic pulmonary arterial hypertension
HRP	horseradish peroxidase
IBMX	3-isobutyl-1-methylxanthine
kb	kilo base pairs
kDa	kilo dalton
Kv	voltage-gated potassium channels
M	molar (mole/litre)
MCT	monocrotaline
MCT-PH	monocrotaline-induced pulmonary hypertensive
mg	milligram
min	minute(s)
ml	milliliter
8mm-IBMX	8-Methoxymethyl-3-isobutyl-1-methylxanthine
mM	millimolar
mRNA	messenger ribonucleic acid
µCi	microcurie
µg	microgram
µl	microliter
µm	micrometer
µM	micromolar
nm	nanometer
nM	nanomolar
NO	nitric oxide
PAGE	polyacrylamide gel electrophoresis
PAH	pulmonary arterial hypertension
Pap	papaverine
PASMCs	pulmonary arterial smooth muscle cells
PBGD	porphobilinogen deaminase

PBS	phosphate-buffered saline
PCR	polymerase chain reaction
PDE	phosphodiesterase
PH	pulmonary hypertension
PKG	protein kinase G
PKA	protein kinase A
PMSF	phenylmethylsulfonyl fluoride
P/S	penicillin/streptomycin
PVRI	pulmonary vascular resistance index
qRT-PCR	quantitative real time-polymerase chain reaction
rpm	revolution per minute
RT-PCR	reverse transcriptase-polymerase chain reaction
RNA	ribonucleic acid
Rnase	ribonuclease
RT	room temperature
RVSA	right ventricular systolic pressure
SAP	systemic arterial pressure
SDS	sodium dodecyl sulfate
sec	second(s)
sGC	soluble guanylyl cyclase
SMC	smooth muscle cell
SM-MHC	smooth muscle-myosin heavy chain
SVRI	systemic vascular resistance index
TAE	tris-acetate EDTA
TBST	tris-buffered saline buffer+ 0.1% Tween 20
TCA	trichloroacetic acid
TEMED	*N*,*N'*,*N'*-tetramethyl-ethane-1,2-diamine
Tris	tris-(hydroxy methyl)-amino methane
UV	ultraviolet
V	volt
VIP	vasoactive intestinal peptide

SUMMARY

Pulmonary arterial hypertension (PAH) is a progressive disease defined by an elevation of pulmonary vascular resistance due to sustained vessel contraction and enhanced vascular remodeling. The abnormal tone and remodeling in the pulmonary vasculature are believed to be related, at least in part, to the decrease of cyclic nucleotide levels that are controlled by cyclic nucleotide phosphodiesterases (PDEs).

PDEs, of which 11 families have been identified, maintain homeostasis of the second messengers by catalyzing the hydrolysis of cAMP and cGMP with diverse compartmentalization and substrate specificities. Interestingly, increased expression of some PDE isoforms has been observed in PAH and beneficial effects of PDE5 inhibitors, PDE1 inhibitors and PDE3/4 inhibitors have been reported in clinical or experimental PAH. The role of PDE7-11 in PAH has not been investigated, thus we aimed to investigate the expression profile of those higher isoforms. In addition, we were interested in the contribution of these enzymes to the pathophysiology of PAH using the well-established monocrotaline (MCT)-induced pulmonary hypertensive rat model.

In this study, a prominent increase of PDE10A expression was observed among the multiple newly identified PDEs (PDE7-11) which are all present in lung tissue. Interestingly, the upregulation of PDE10A is specific in the pulmonary vasculature of pulmonary hypertensive subjects without significant changes in the systemic vasculature such as aorta or femoral artery.

As one of the most recently described PDEs, PDE10A is characterized as a cAMP-PDE and a cAMP-inhibited cGMP-PDE. Research on PDE10 is mainly focused on neurological studies because of its abundant expression in the brain. We demonstrated for the first time the predominant localization of PDE10A in the media of the small pulmonary arteries and nuclear compartmentalization in pulmonary arterial smooth muscle cells (PASMCs). In accordance, both PDE10A expression and cAMP hydrolyzing activity are remarkably increased in PASMCs from MCT-induced PH rats as compared to control rats, suggesting a

contribution of PDE10A to the proliferative phenotype of PASMCs in the process of PH. Futher more, PDE10A immunoreactivity is strongly increased in pulmonary arteries of IPAH patient lung sections as compared to the donors, indicating clinical relevance of the findings obtained from the MCT model.

The anti-proliferative effect of PDE10 inhibition is proved to be largely relevant to an increase of intracellular cAMP levels that may subsequently alter downstream signaling events such as phosphorylation of the cAMP response element binding protein (CREB). In our investigation, we found that inhibition of PDE10A by employing a selective inhibitor of PDE10 (papaverine) or PDE10A specific small interfering RNA (siRNA) promoted intracellular cAMP generation, induced CREB phosphorylation and attenuated proliferation of PASMCs from MCT-induced PH rats.

Furthermore, treating MCT-PH rats with the PDE10 inhibitor papaverine for 14 days by intravenous infusion markedly reduced right ventricular systolic pressure values as well as total pulmonary vascular resistance index, without effects on the systemic arterial pressure. In addition, the percentage of fully muscularized peripheral pulmonary arteries was significantly decreased.

Taken together, this study supports a central role of PDE10A in progressive pulmonary vascular remodeling and suggests a novel therapeutic opportunity for the treatment of pulmonary arterial hypertension.

ZUSAMMENFASSUNG

Die pulmonal-arterielle Hypertonie (PAH) ist durch einen zunehmend ansteigenden Gefäßwiderstand definiert, welcher durch dauerhafte Kontraktion kleiner Pulmonalarterien und ein verstärktes vaskuläres Remodeling zu einem Anstieg des Blutdrucks im Lungenkreislauf führt. Diese pathologischen Veränderungen der Pulmonalgefäße werden u.a. auf ein geringeres Vorhandensein der zyklischen Nukleotide cAMP und cGMP zurück geführt, was maßgeblich durch die Aktivität zyklischer Nukleotid- Phosphodiesterasen (PDEs) bestimmt wird.

Die Familie der PDEs umfasst derzeit 11 Mitglieder. Sie hydrolysieren cAMP und cGMP zu AMP bzw. GMP und haben durch ihre zelluläre und intrazelluläre Verteilung und Substratspezifität einen bedeutenden Einfluss auf die Homöostase dieser second messenger. Sowohl in experimenteller PAH als auch in klinischen PAH-Studien konnte bereits gezeigt werden, dass eine erhöhte Expression bestimmter PDEs vorliegt und dass die Behandlung mit PDE5-, PDE1- und PDE3/4-Inhibitoren gefäßerweiternd wirkt und zudem einen antiproliferativen und antimigrativen Effekt auf vaskuläre Zellen hat. Die Rolle der PDEs 7 bis 11 in PAH ist bisher jedoch noch unzureichend erforscht. Daher war unser Ziel heraus zu finden, ob Mitglieder dieser PDEs in der Pathophysiologie der PAH eine Rolle spielen. Für diese Untersuchungen diente uns das bereits etablierte experimentelle Modell der Monocrotalin (MCT) - induzierten pulmonalen Hypertonie in der Ratte.

Bei der Untersuchung der PDE-Expression im Lungengewebe zeigte sich neben der Expression der PDEs 7 bis 9 und der PDE11 eine deutlich erhöhte Expression der PDE10A. Diese konnte zudem spezifisch in der verdickten und veränderten Gefäßmuskulatur der Pulmonalarterien immunhistochemisch lokalisiert werden. In systemischen Gefäßen wie der Aorta oder der Femoralarterie konnten jedoch keine signifikanten Veränderungen in der PDE10A-Expression festgestellt werden.

Als eine der erst kürzlich beschriebenen PDEs wird die PDE10A als cAMP-PDE und als cAMP-inhibierte cGMP-PDE bezeichnet und wird wegen ihres Vorkommens im Gehirn hauptsächlich in neurologischen Studien untersucht. In dieser Arbeit konnten wir erstmalig zeigen, dass die PDE10A eine vorherrschende Expression in der Media kleiner Pulmonalarterien aufweist und in pulmonal-arteriellen glatten Muskelzellen (PASMCs) überwiegend nukleär lokalisiert ist. Im Vergleich zu Kontroll-PASMCs ist sowohl die Expression als auch die cAMP-hydrolysierende Aktivität der PDE10A in PASMCs aus MCT-injizierten Ratten deutlich erhöht, was eine Mitwirkung der PDE10A bei der Proliferation der PASMCs und dem Fortschreiten der PAH vermuten lässt. Desweiteren ist die PDE10A Immunoreaktivität in pulmonalen Arterien der untersuchten Lungenbereiche von IPAH Patienten im Vergleich zu denen der Spender stark erhöht, was darauf hinweist, daß eine klinische Relevanz dieser Ergebnisse, die vom MCT Modell gezeigt wurden vorliegt.

Phosphodiesterase-Inhibitoren führen meist zu einer Erhöhung der intrazellulären cAMP-Konzentration, was im Folgenden Auswirkungen auf den Phosphorylierungsstatus und somit die Aktivität von Transkriptionsfaktoren wie CREB (cAMP response element binding protein) hat. Unsere Untersuchungen zeigten, dass die Hemmung der PDE10A durch Verabreichen des Inhibitors Papaverin oder durch die Verwendung PDE10A-spezifischer kleiner einzelsträngiger RNAs (siRNAs) zu einer gesteigerten intrazellulären cAMP-Konzentration führt, die Phosphorylierung von CREB induziert und die Proliferation von PASMCs aus MCT-injizierten Ratten mit PAH vermindert. Überdies wird die PASMC-Proliferation, verglichen mit der Hemmung weiterer cAMP-abbauender PDEs, am meisten durch Inhibition der PDE10A verringert.

Die Behandlung von MCT-PH-Ratten mit dem PDE10A Inhibitor Papaverin für 14 Tage per intravenöse infusion reduzierte deutlich den systolischen Druck des rechten Ventrikels ebenso wie den gesamten pulmonal-vaskulären Widerstand, ohne den systemische Blutdruck zu beeinflussen. Ebenso war der Prozentsatz von voll muskularisierten peripheren pulmonalen Arterien deutlich durch diesen therapeutischen Ansatz gehemmt.

Zusammenfassend deuten diese Ergebnisse darauf hin, dass die PDE10A eine zentrale Rolle im vaskulären Remodeling-Prozess einnimmt und daher ein therapeutisches Ziel zur Behandlung von pulmonaler Hypertonie darstellen könnte.

1 INTRODUCTION

1.1 Pulmonary hypertension (PH)

Pulmonary hypertension is a fatal disease which is clinically characterized by a progressive rise in pulmonary vascular pressure. When untreated, right ventricle overload leads to right ventricular hypertrophy and in the end stage right heart failure and death with an average survival time as short as 2.8 years[1]. Pulmonary hypertension has a multifactorial pathobiology. Moreover, available therapies for PH were shown to improve the prognosis, but not to cure the disease.

1.1.1 Definition of pulmonary hypertension

The first description came from autopsy specimens more than a century ago by a German physician- Ernst von Romberg[2], and until 1951 the first clinical and hemodynamic study was made ante mortem[3]. In pulmonary hypertension the average pressure in the pulmonary artery is higher than 25 mmHg at rest or 30 mmHg during physical activity, while the pressure in a normal pulmonary artery is about 15 mmHg at rest[4].

1.1.2 Classification of pulmonary hypertension

Pulmonary hypertension was initially classified into two categories including primary pulmonary hypertension and secondary pulmonary hypertension[5], simply based on the presence or absence of identifiable causes. With more understanding of the disease, the classification of PH has gone through a series of changes. The latest and probably the best classification up to now is the Dana Point Classification made on the 4th World Symposium on PH held in 2008 in Dana Point, California, which divided the PH into five groups[6] (Figure 1) that shared similar pathophysiologic mechanisms and clinical presentation as well as therapeutic approaches.

Tabel 1: Updated classification of PH (Dana Point, 2008)

1. Pulmonary arterial hypertension (PAH)
1.1. Idiopathic PAH 1.2. Heritable 1.2.1. BMPR2 1.2.2. ALK1, endoglin (with or without hereditary hemorrhagic telangiectasia) 1.2.3. Unknown 1.3. Drug- and toxin-induced 1.4. Associated with 1.4.1. Connective tissue diseases 1.4.2. HIV infection 1.4.3. Portal hypertension 1.4.4. Congenital heart diseases 1.4.5. Schistosomiasis 1.4.6. Chronic hemolytic anemia 1.5 Persistent pulmonary hypertension of the newborn
1'. Pulmonary veno-occlusive disease (PVOD) and/or pulmonary capillary hemangiomatosis (PCH)
2. Pulmonary hypertension owing to left heart disease
2.1. Systolic dysfunction 2.2. Diastolic dysfunction 2.3. Valvular disease
3. Pulmonary hypertension owing to lung diseases and/or hypoxia
3.1. Chronic obstructive pulmonary disease 3.2. Interstitial lung disease 3.3. Other pulmonary diseases with mixed restrictive and obstructive pattern 3.4. Sleep-disordered breathing 3.5. Alveolar hypoventilation disorders 3.6. Chronic exposure to high altitude 3.7. Developmental abnormalities
4. Chronic thromboembolic pulmonary hypertension (CTEPH)
5. Pulmonary hypertension with unclear multifactorial mechanisms
5.1. Hematologic disorders: myeloproliferative disorders, splenectomy 5.2. Systemic disorders: sarcoidosis, pulmonary Langerhans cell histiocytosis: lymphangioleiomyomatosis, neurofibromatosis, vasculitis 5.3. Metabolic disorders: glycogen storage disease, Gaucher disease, thyroid disorders 5.4. Others: tumoral obstruction, fibrosing mediastinitis, chronic renal failure on dialysis

1.1.3 Histology and concepts of pulmonary arterial hypertension (PAH) pathology

1.1.3.1 Histology and pathology

The common histological features in PAH are the remodeling of all three layers of the pulmonary vasculature (intimal, medial and adventitia layer) as well as the formation of plexiform lesion (Figure 1)[4].

A) **B)**

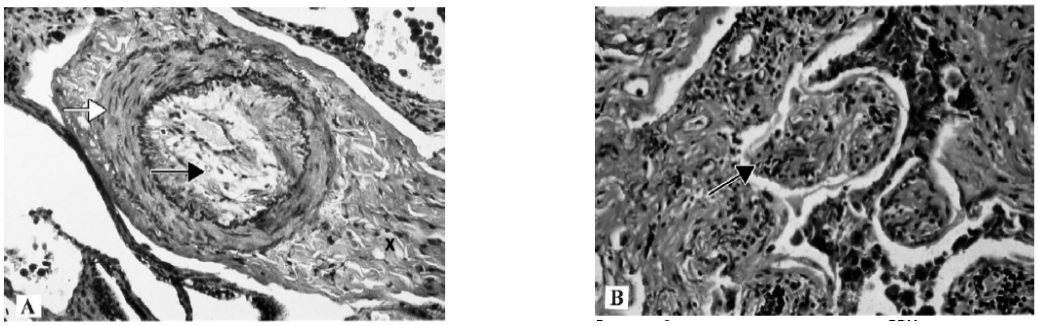

Figure 1: Histology of PAH. A) Muscular pulmonary artery from a PAH patient with medial hypertrophy (white arrow), luminal narrowing by intimal proliferation (black arrow), and proliferation of adventitia (X). **B)** Characteristic plexiform lesion from an obstructed muscular pulmonary artery (black arrow). (Gaine, S. P. & Rubin L. J., 1998)[4]

The abnormalities of the pulmonary vasculature comprise 1) medial hypertrophy of large pulmonary arteries and muscularization of distal precapillary arteries; 2) proliferation in the adventitia of small pulmonary arteries and arterioles; 3) intimal hyperplasia that is particularly occlusive in vessels at 100–500 μM; 4) plexiform lesions of arterial branches distal to an obstructed larger artery; 5) loss of precapillary arteries[7, 8] (Figure 2).

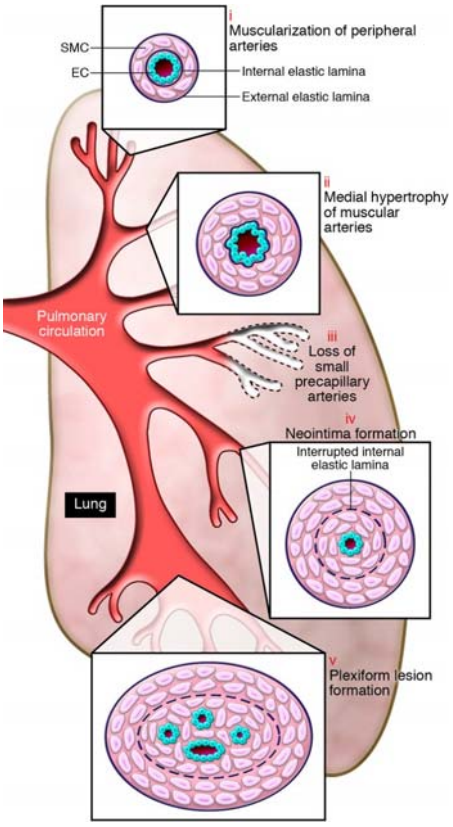

Figure 2: Scheme of pathological abnormalities in PH throughout the pulmonary circulation. (Rabinovitch,M.,2008)[7]

1.1.3.2 Molecular and cellular regulators

Diverse stimuli like inflammation, shear stress and hypoxia lead to 1) vasoconstriction, due to the imbalance between vasodilators and vasoconstrictors; 2) vascular remodeling, resulting from the imbalance between mitogenic and anti-mitogenic mediators; 3) in situ thrombosis caused by abnormalities of blood coagulation factors and fibrinolytic factors[9, 10], all of which result in increased pulmonary pressure in PAH. Recent pathophysiologic studies have addressed evidences on a couple of key factors mediating the process of PAH, among which nitric oxide, prostacyclin, vasoactive intestinal peptide, Endothelin-1, potassium channels and serotonin[11-13] are widely investigated.

1.3.3.2.1 Nitric oxide

Over the past decades, nitric oxide (NO), which is synthesized by a family of NO synthase enzyme (NOS) from the amino acid L-arginine in endothelial cells, is believed to be a vasodilator targeting SMC on soluble guanylyl cyclase

(sGC)/vasorelaxation pathway. The activation of sGC in SMCs leads to cGMP accumulation and consequently PKG activation and reduction of intracellular calcium, which leads to vasodilation. Cyclic GMP is removed by phosphodiesterases (PDEs). Diminished eNOS expression in pulmonary vasculature has been demonstrated in PH patients, particularly in IPAH patients[14]. Furthermore, eNOS-null mice are more susceptible to stimuli that trigger pulmonary hypertension as compared to the wild-type mice[15, 16], suggesting that NO not only acts as a vasodilator, but also inhibits smooth muscle cell proliferation[17] and platelet aggregation[18]. All of these factors indicates that NO plays an important role in PAH.

1.3.3.2.2 Prostacyclin and thromboxane A2

Prostacyclin is an arachidonic acid metabolites, and is synthesized in endothelial cells by prostacyclin synthase. It is a vasodilator and can prevent vascular SMC proliferation and platelet aggregation via adenylate cyclase (AC)/cAMP-dependent pathways. Thromboxane A2 is produced by endothelial cells and platelets and increases vasoconstriction and activates platelets[19]. In patients with PAH, decreased level of prostacyclin accompanied by increased level of thromboxane A2 were observed by urine analysis[20]. Correspondingly, expression of prostacyclin synthase is reduced in small and medium-sized pulmonary arteries in PAH patients[21]. Therefore the imbalance between prostacyclin and thromboxane A2 favours vasoconstriction, thrombosis, as well as vessel wall remodeling associated with PAH development.

1.3.3.2.3 Vasoactive intestinal peptide (VIP)

Decreased VIP immunoreactivity in serum and lung tissue, shown in IPAH patients, may contribute to the pathogenesis of PAH considering its potential roles as a pulmonary vasodilator and an inhibitor of PASMC proliferation and platelet aggregation[22]**.** $VIP^{-/-}$ mice exhibit spontaneous PAH in the absence of hypoxia and VIP may act as an endogenous modulator of calcineurin-NFAT (nuclear factor of activated T cells) transcriptional activation[23, 24]. It is also demonstrated that VIP may act through its receptors in vasculature to activate cAMP and cGMP systems[22], but the key mechanisms involved are unclear.

1.3.3.2.4 Endothelin-1 (ET-1)

ET-1 is predominantly produced by endothelial cells and is a potent vasoconstrictor. In addition, it acts as mitogen that promotes inflammation and SMC proliferation. Elevated ET-1 levels in lung and circulation are reported from rats with hypoxia-induced PAH[25] and from PAH patients[26], which strongly supports the concept that the endothelin system plays a crucial role in the development of PAH. The effects of ET-1 in the lung are complex and depend on two different ET-1 receptors named ETA and ETB. ETA presents mainly in SMCs while ETB locates in both SMCs and endothelia cells[27]. Through its action on ETA and ETB in PASMCs, ET-1 evokes Ca^{2+} sparks in PASMCs via activation of phospholipase C and consequently causes vasoconstriction and sustained activation of protein kinase C, which mediates mitogenic actions[28, 29]**.** In contrast to the activation of ETB in PASMCs, ET-1 activates the endothelial ETB receptor, which leads to the release of vasodilator and antiproliferative agents like NO and prostacyclin[30] and promotes clearance of circulating ET-1[31] in pulmonary vasculature.

1.3.3.2.5 Potassium channels

Reduced expression and function of voltage-gated potassium channels (Kv), notably Kv1.5 and Kv2.1, was observed in PASMCs either from IPAH patients[32] or from rats with hypoxia-induced PAH[33]**.** The selective loss of these Kv channels on PASMCs leads to membrane depolarization, sustained increase of the intracellular calcium by Ca^{2+} influx, and promotes both vasoconstriction and cell proliferation.

1.3.3.2.6 Serotonin

Serotonin (5-HT, 5-hydroxytryptamine) is considered as both a vasoconstrictor[34] and a mitogen that promotes smooth muscle cell hypertrophy[35]. Elevated 5-HT in plasma was observed in IPAH patients. More recently, a number of studies showed that the 5-HT transporter (5-HTT) and 5-HT receptors in the pulmonary vasculature are increased in both clinical and experimental PAH[36, 37]. In mice, selective 5-HTT inhibitors protect against hypoxic pulmonary hypertension[38]; while transgenic 5-HTT overexpression in smooth muscle results in PH[39].

1.1.4 Pharmacological and clinical therapies

Major pharmacological therapies include therapy with vasodilators and more recently therapy with agents targeting pulmonary vascular remodeling. To maximize therapeutic benefits and minimize side effects, combination therapy with existing drugs under different mechanisms of action is essential.

1.1.4.1 Prostacyclin

Prostacyclin analogues promote vasodilation as well as inhibit vascular proliferation and platelet aggregation[40]. Intravenous epoprostenol was the first approved approach to improve the symptoms and survival of PAH patients[41, 42]. Because of the short half-life of epoprostenol, longer-active prostacyclin alternatives such as iloprost and treprostinil with the same or better efficacy and less side effects have been developed in clinical trial for intravenous, subcutaneous or inhaled treatment of PAH[43-46].

1.1.4.2 Inhaled NO and sGC stimulators

Inhaled NO, being delivered directly to pulmonary resistance vessels, has been proven to be a potent and selective pulmonary vasodilator with minor systemic effects[47] via NO-sGC-cGMP pathway. Since long-term use of Inhaled NO is limited by its short half-life, drugs that activate sGC in a NO-independent manner are considered as innovative alternatives to direct NO donors[48]. Recently several compounds have shown beneficial effects on vasodilation and vessel remodeling via inhalation in experimental PAH animals[49, 50]. Moreover, riociguat (BAY 63-2521), a sGC stimulator, was reported to improve pulmonary hemodynamic parameters and cardiac index to a greater extend than inhaled NO in PAH patients[51].

1.1.4.3 Endothelin antagonists

ET-1 acts as an important vasoconstrictor and mitogen in the development of PAH. Pharmacologic antagonists against ET-1 receptors with variable specificities are under a widespread investigation for PAH treatment. Oral bosentan, a dual endothelin receptor antagonist, improves hemodynamics and exercise capacity, as well as survival of PAH patients[52, 53]. However bosentan has been reported to cause liver dysfunction in a great percentage of patients.

While ETA specific antagonists consisting of sitaxsentan[54] and ambrisentan[55] both improve exercise capacity of PAH patients in clinical trails, with a low incidence of hepatic toxicity.

1.1.4.4 Phosphodiesterase 5 (PDE5) inhibitors

Sildenafil was initially used for erectile dysfunction and subsequently proved to be a therapeutic candidate for PAH based on the high abundant expression of PDE5 in pulmonary vasculature as compared to systemic vasculature[56, 57]. By inhibiting the breakdown of cGMP, sildenafil can augment the NO-sGC-cGMP signaling in pulmonary vasculature, resulting in pulmonary vasodilation and inhibition of SMC proliferation. Beneficial effects including improved symptoms, hemodynamics, exercise capacity and survival have been shown by a one-year extension study after a daily oral treatment with sildenafil for 12 weeks[57].

1.1.4.5 Tyrosine kinase inhibitors

Platelet-derived growth factor (PDGF), as a growth factor, induces cell proliferation and migration. In an experimental PH model, PDGF and its receptors are increased and by applying imatinib, a multi-inhibitor for tyrosine kinase, the pulmonary vascular remodeling process was reversed[58]. Furthermore, beneficial effects of imatinib on PAH patients have also been shown in three cases of clinical trails[59-61]. But more evaluations with much larger number of PAH patients are required in randomized clinic studies.

1.2 Phosphodiesterases (PDEs)

1.2.1 Cyclic nucleotides (cAMP and cGMP)

Adenosine 3', 5-cyclic monophosphate (cAMP) and guanosine 3', 5'-cyclic monophosphate (cGMP) have been defined as second messengers half a century ago[62]. Both cAMP and cGMP play critical roles in various tissues by regulating diverse signaling pathways in multidimension, not only because of their time-dynamic presenting, also due to their subcellular compartmentalization[63]. Extracellular signaling is translated into changes of cAMP and cGMP via different membrane receptors, which subsequently lead to multiple cell responses by coordinated activation of cyclic nucleotide-dependent protein kinases (PAK and PKG). In the case of the vasculature, they regulate

the vascular tone as well as the smooth muscle cell growth[64]. Physiologically, intracellular levels of cAMP and cGMP are controlled in homeostasis between their rate of synthesis by adenylyl and guanylyl cyclases and their rate of hydrolysis by cyclic nucleotide PDEs respectively[63-65](Figure 3).

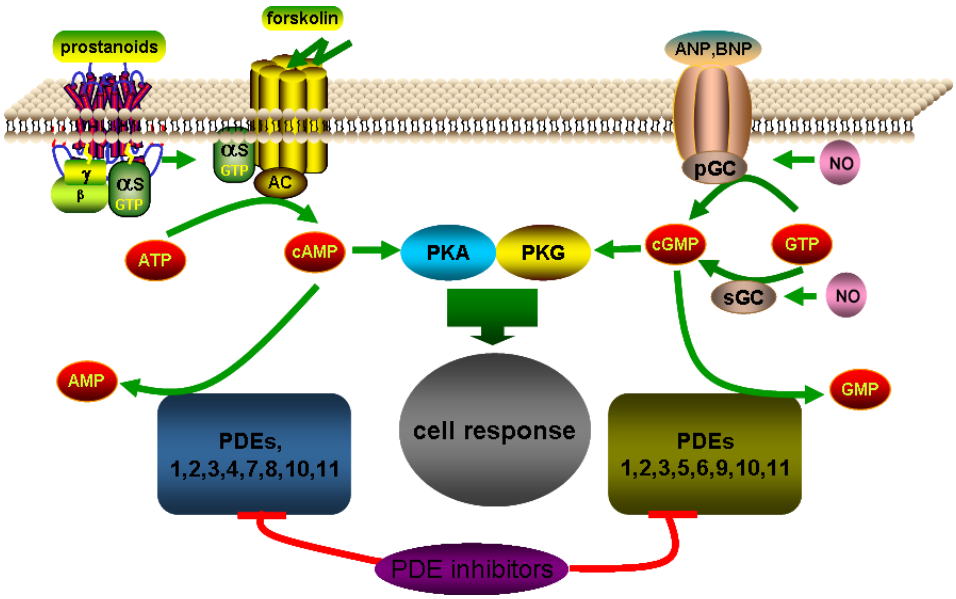

Figure 3: cAMP and cGMP signaling pathway. Prostacyclin, forskolin, arterial natriuretic peptide (ANP), brain natriuretic peptide (BNP) and NO, activate adenylate cyclase (AC) or guanylate cyclase (GC) to generate cAMP and cGMP from ATP or GTP. The intracellular second messenger cAMP and cGMP activate protein kinases (PKA and PKG), which phosphorylate downstream proteins and induce cellular responses. Phosphodiesterases (PDEs) counter the effects of the stimuli by degrading cAMP and cGMP into 5'AMP and 5'GMP. (Modified from Schermuly R.T., 2005)

1.2.2 Cyclic nucleotide PDEs

PDEs are a superfamily of enzymes that catalyze the hydrolysis of 3',5'-cyclic nucleotides (3',5'-cAMP/cGMP) to the corresponding nucleotide 5'-monophosphates (5'-AMP/GMP)[66] (Figure 4). Both cAMP and cGMP are tightly regulated by the differentially distributed PDE isoforms in cells to maintain physiological functions.

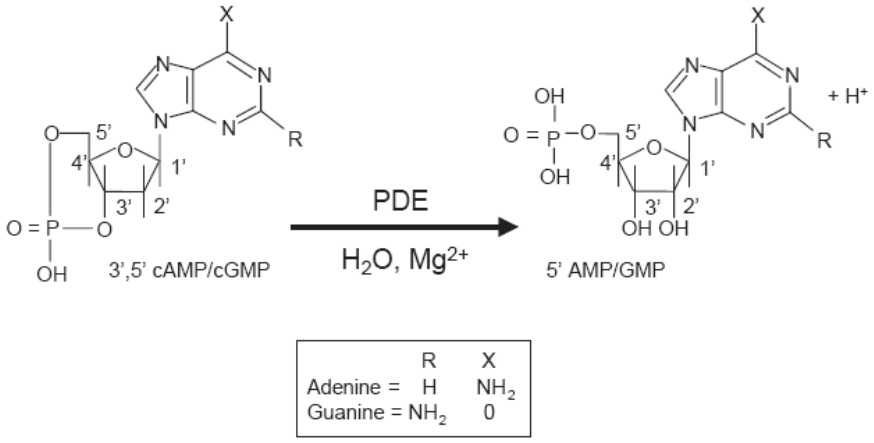

Figure 4: Cyclic nucleotide hydrolysis by PDEs. (Lugnier, C., 2006)[66]

1.2.2.1 PDE classification

To date, with 21 genes encoding PDEs identified in the human genome, PDEs are subdivided into 11 isoforms (PDE1-PDE11) bases on their amino acid sequences, substrate specificities, kinetics, allosteric regulators and inhibitor sensitivities[63] (Figure 5).

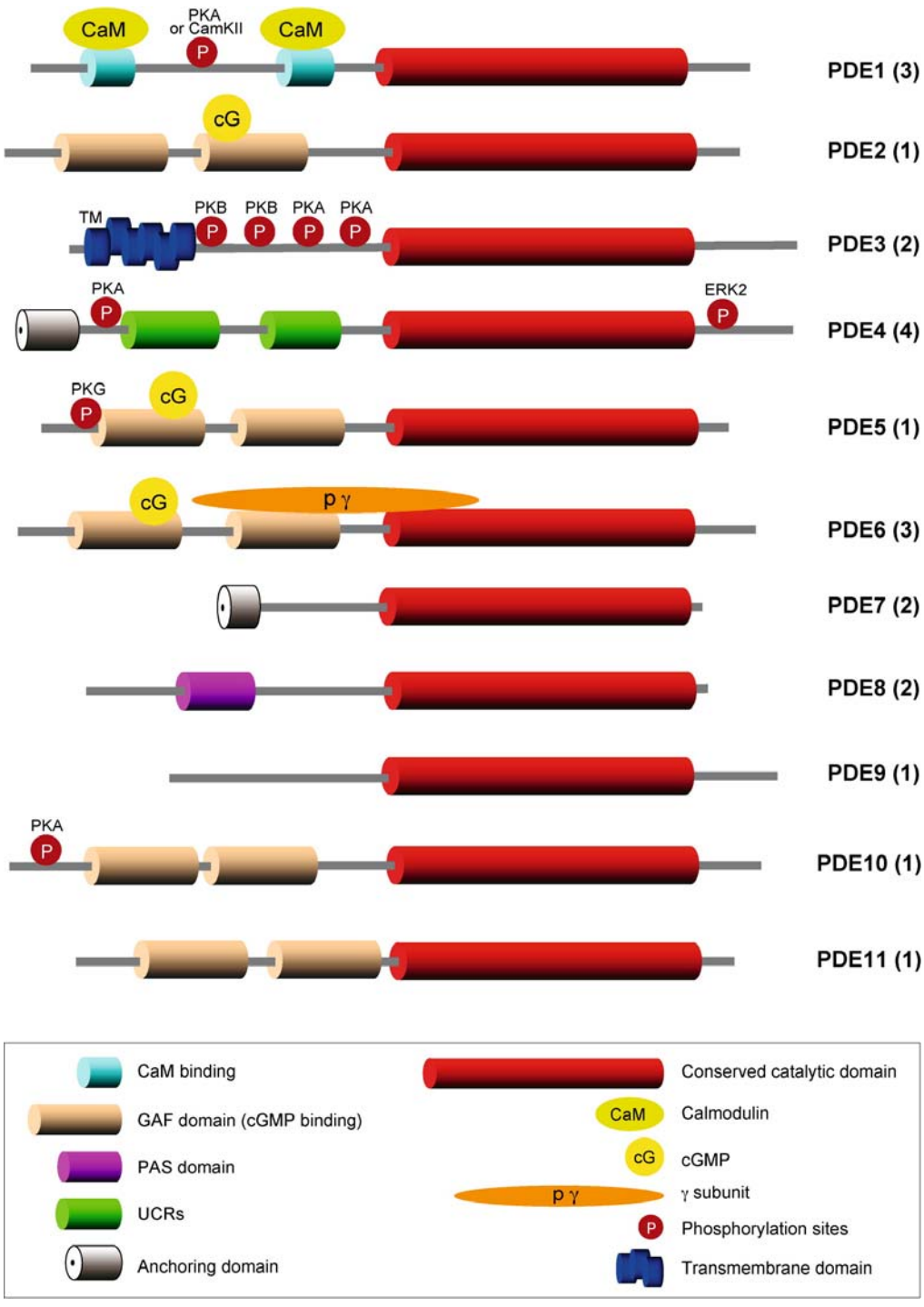

Figure 5: Structure of PDE families. The number in parenthesis presents the number of genes composing the subfamily. (Conti M & Beavo J. 2007)[63]

Among those PDEs, PDE4, PDE7, and PDE8 selectively hydrolyze cAMP; PDE5, PDE6, and PDE9 are selective for cGMP, while 5 other subfamilies (PDE1, 2, 3, 10, and 11) hydrolyze both cyclic nucleotides with varying efficiency[63, 65-68] (Table 2).

Table 2. Characteristics and distribution of PDEs (Modified from Siuciak J.A., 2006)

Family	Substrate	Property	Tissue expression	Inhibitors
PDE1A PDE1B PDE1C	cAMP / cGMP cAMP / cGMP cAMP / cGMP	Ca2+ /CAM-activated	Brain, heart, smooth muscle, skeletal muscle	8-Methoxymethyl IBMX, Vinpocetine
PDE2A	cAMP / cGMP	cGMP-activated	Broadly distributed, high in heart, lower in brain	EHNA
PDE3A PDE3B	cAMP / cGMP	cGMP-inhibited, Phosphorylation	Cardiac muscle, adipose tissue,vascular smooth muscle, pancreas, platelets	Cilostamide, Milrinone,
PDE4A PDE4B PDE4C PDE4D	cAMP	UCR1/UCR2 regions, Phosphorylation	Broadly distributed, brain, inflammatory cells, lung, cardiac myocyte	Rolipram,Roflumilast
PDE5A	cGMP	Phosphorylation, cGMP	Lung, platelets, vascular smooth muscle, testis	Sildenafil, Tadalafil, Vardenafil, Zaprinast
PDE6A PDE6B PDE6C	cGMP	Phosphorylation, cGMP, Trasnsducin	Rods and cones	Sildenafil, Tadalafil, Vardenafil, Zaprinast
PDE7A PDE7B	cAMP	Rolipram-insensitive	Skeletal muscle, immune cells, brain, kidney, heart	
PDE8A PDE8B	cAMP	Rolipram-insensitive, IBMX-insensitive	Testis, liver, kidney, eye, heart, brain, skeletal muscle	Dipyridamole
PDE9A	cGMP	IBMX-insensitive	Kidney, liver, lung, heart	Sildenafil, Zaprinast
PDE10A	cAMP / cGMP	cAMP-Inhibited	Brain, testis, lung, pancreas	Papaverine
PDE11A	cAMP / cGMP	cGMP-activated	Skeletal muscle, prostate, testis	Dipyridamole

1.2.2.2 PDE10

PDE10 is one of the most recently described PDEs and was originally characterized as a single member of a dual-substrate gene family in 1999 from rodent as well as from human brain[69-72]. PDE10 transcripts were particularly abundant in brain, thyroid and testis. PDE10A is the only isoform of PDE10 subfamily and contains a consensus PDE catalytic domain in the C-terminus and two GAF domains in the N-terminus (Figure 6)[69, 70]. Different from the GAF domain of other PDE families, the GAF domain of PDE10A is the only one that binds to cAMP instead of cGMP, which may contribute to the allosteric stimulation of PDE10A[73, 74].

Figure 6: Structure of PDE10A.

Existing in multiple splice variant forms, PDE10A has the capacity to hydrolyze both cAMP and cGMP; however it has higher affinity for cAMP and is more efficient with cAMP as the substrate. The Km for cAMP is approximately 0.05 µM, whereas the Km for cGMP is 3 µM. In addition, the Vmax for cAMP hydrolysis is fivefold lower than for cGMP[70]. Because of this kinetic pattern, cGMP hydrolysis by PDE10A is potently inhibited by cAMP *in vitro*, suggesting that PDE10A functions as a cAMP-PDE and a cAMP-inhibited cGMP-PDE *in vivo*[69-71]. Papaverine (Figure 7), a naturally occurring plant alkaloid and smooth muscle relaxant, can be used as a potent inhibitor of PDE10 exhibiting a low Ki of 17 nM as compared to PDE3A/B (Ki = 279 and 417 nM, respectively)[75].

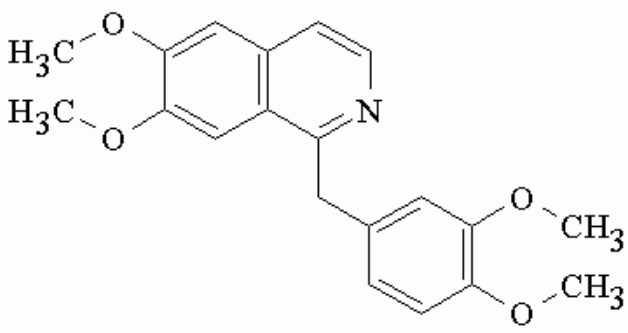

Figure 7: Structure of papaverine.

1.2.2.3 Pathophysiological roles of PDEs in PAH and inhibitors

Given the intricate expression patterns in distinct tissues and cells, each member of PDE family participates in discrete pathophysiological processes such as penile erection, asthma, pulmonary hypertension, atherosclerosis, heart failure, and inflammation. Furthermore, subcelluar compartment of PDEs leads to diverse signal transduction pathways in a space-dynamic and time-dynamic manner. Therefore, other than fundamental concerns, PDEs are of great pharmacological interest[64].

Because of the crucial regulation role of cyclic nucleotides in signaling transduction, the concept that PDEs are involved in the pathological process of PAH is widely accepted[76]. Interestingly, expression and activities of PDEs were reported to be altered in both experimental and human PAH[77]. Expression profiling of single member of the PDE super family in healthy and remodeled pulmonary vasculature revealed that PDE1, PDE3 and PDE5 isoforms are differentially regulated[78-81]. In preclinical and clinical studies we have shown that the inhibition of PDE1 by 8MM-IBMX[78] and PDE5 by sildenafil[57, 80] stabilizes the second messenger signaling and regulates vascular remodeling, vascular tone and optimization of gas exchange. Moreover, in MCT-induced PH rats, inhibition of PDE3 and PDE4 isoforms was found to partly reverse the pathological inward remodeling in PH[82, 83]. Given that higher PDEs (PDE7-11) were defined more recently, further investigations should be performed to understand the possible involvements of higher PDEs in PAH and to improve the therapy of PAH by pharmacological PDE inhibitors.

2 AIMS OF THE STUDY

In the pulmonary vasculature, PDEs modulate various signaling pathways via the tight control of the cyclic nucleotides. Expression of PDEs is altered in PAH and inhibitors of PDEs suppress pulmonary vascular remodeling, while the role of the most newly identified PDEs (PDE7-11) has not been investigated yet. The substrate specificity, as well as the cellular and subcellular distribution, of these newly identified PDEs may provide additional exciting insights in the pathophysiology of PAH. Our aim was to identify and characterize cellular functions of previously newly identified PDEs in pulmonary vascular remodeling in PAH and to offer new selective therapy targets for PAH. In this study, a series of study were undertaken as follows:

1. Gene expression pattern of newly identified PDEs both in lung tissue and primary PASMCs from control and MCT-induced PH rats.
2. Changes in enzyme activity as well as localization of the candidate PDE in the lung and PASMCs from control and MCT-induced PH rats.
3. *In vitro* effects of inhibiting the candidate PDE by siRNA and the pharmacological inhibitor.
4. Molecular mechanisms which may be involved in affecting the cellular responses after inhibition of the candidate PDE.
5. Therapeutic effects of the candidate PDE inhibitor on pulmonary hemodynamics and remodeling of MCT-induced PH rats.
6. Expression and localization of PDE10A in donors and IPAH lungs.

3 MATERIALS AND METHODS

3.1 Materials

3.1.1 Chemicals, reagents and kits

Most of the chemicals were purchased either from Sigma-Aldrich (USA) or from Merck (Germany). The rests are listed as follows.

Product	**Company**
Baytril (quinolone antibiotic)	Bayer, Gemany
Bovine serum albumin powder	Serva, Germany
Bovine serum albumin solution (2 mg/ml)	Bio-Rad, USA
cAMP EIA kit	Cayman Europe, Estonia
[^{3}H]-cAMP	Amersham, USA
DAPI	Dakocytomation, USA
D_c protein assay kit	Bio-Rad, USA
DEPC water	Roth, Germany
Digest All 2 (trypsin)	Vector, UAS
Domitor (Medetomidinhydrochlorid, 100 mg/ml)	Pfizer, USA
DNA Ladder (100 bp, 1 kb)	Promega, USA
Enhanced chemiluminescence (ECL) kit	Amersham, USA
Fluorescent mounting medium	Dakocytomation, USA
GoTaq® PCR Core System I	Promega, USA
ImProm-II™ Reverse Transcription System	Promega, USA
Ketavet (Ketaminhydrochlorid, 100 mg/ml)	Pharmacia, USA
Milk powder	Roth, Germany
N,N'-Methylene-bis-Acrylamide solution, Rotiphorese gel 30	Roth, Germany
NovaRED substrate kit	Vector, USA
Protein rainbow markers	Amersham, USA
QAE Sephadex A-25	Amersham, USA
RIPA buffer	Santa Cruz, USA
RNase Away	Molecular Bioproducts, USA
Saline (NaCl 0.9%)	B. Braun, Germany
Scintillation solution (Rotiszint®eco plus)	Roth, Germany

SDS Solution, 10% w/v	Promega, USA
Sildenafil	Pfizer, USA
SYBR® GreenER™ qPCR SuperMixes Universal kit	Invitrogen, USA
[^{3}H]-thymidine (1 mCi/ml)	Amersham, USA
Tris-HCl 0.5 M, pH 6.8	Amresco SOLON, USA
Tris-HCl 1.5 M, pH 8.8	Amresco SOLON, USA
Trizol	Invitrogen, USA
UltraPure water	Cayman Europe, Estonia
X-tremeGENE siRNA Transfection Reagent	Roche, Germany

3.1.3 Cell culture medium

DMEM/F12, Opti-MEM and HBSS are purchased from Invitrogen (USA). Fetal bovine serum is from Biowest (Germany). The rest including PBS, L-glitamine, penicillin/streptomycin and Trypsin/EDTA are all purchased from PAN (Germany).

3.1.4 Antibodies

Primary antibody	**Company**
Mouse anti-αSMA monoclonal antibody	Sigma-Aldrich, USA
Mouse anti-GAPDH monoclonal antibody	Sigma-Aldrich, USA
Rabbit anti-PDE10A polyclonal antibody	Novus, USA
Rabbit anti-PDE10A polyclonal antibody	Scottish Biomedical, UK
Rabbit anti-CREB polyclonal antibody	Millipore, USA
Rabbit anti-p-CREB (Ser133) polyclonal antibody	Millipore, USA

HRP-conjugated secondary antibody	**Company**
Rabbit anti-mouse IgG	Sigma-Aldrich, USA
Goat anti-rabbit IgG	Pierce, USA

Fluor-conjugated secondary antibody	**Company**
Alexa Fluor® 488 goat anti-rabbit IgG	Invitrogen, USA
FITC conjugated goat anti-rabbit IgG	Invitrogen, USA

3.1.5 Oligonucleotides

Small interfering RNA (siRNA)

siRNA pairs were designed and purchased from Eurogentec (Belgium). The siRNA duplex is made of two strands of 19 complementary RNA bases with 3'dTdT overhangs (Table 3). The negative control si-scramble is a duplex with a random sequence which does not march to any genes.

Table 3: Sequence for PDE10 siRNA pair

Gene		siRNA Sequence
rat PDE10A	Sense strand	5´ GGACAGCUUGGAUUCUACA 3´
	Antisense strand	5´ UGUAGAAUCCAAGCUGUCC 3´

Primers

Primer oligonucleotides were all purchased from Metabion (Germany). The sequences for realtime-PCR are listed in Table 4 and the sequences for standard PCR are listed in Table 5.

Table 4: Primer sequences for quantitative realtime-PCR

Gene (rat)		Primer Sequence
PDE1A 113bp	Forward	5´ ATCAGCCACCCAGCCAAA 3´
	Reverse	5´ GGAGAAAACGGAAGCCCTAA 3´
PDE3A 123bp	Forward	5´ CACAAGCCCAGAGTGAACC 3´
	Reverse	5´ TGGAGGCAAACTTCTTCTCAG 3´
PDE3B 103bp	Forward	5´ GTCGTTGCCTTGTATTTCTCG 3´
	Reverse	5´ AACTCCATTTCCACCTCCAGA 3´
PDE7A 85bp	Forward	5´ GAAGAGGTTCCCACCCGTA 3´
	Reverse	5´ CTGATGTTTCTGGCGGAGA 3´
PDE7B 99bp	Forward	5´ GGCTCCTTGCTCATTTGC 3´
	Reverse	5´ GGAACTCATTCTGTCTGTTGATG 3´
PDE8A 97bp	Forward	5´ TGGCAGCAATAAGGTTGAGA 3´
	Reverse	5´ CGAATGTTTCCTCCTGTCTTT 3´
PDE8B 147bp	Forward	5´ CTCGGTCCTTCCTCTTCTCC 3´
	Reverse	5´ AACTTCCCCGTGTTCTATTTGA 3´
PDE9A 107bp	Forward	5´ GTGGGTGGACTGTTTACTGGA 3´
	Reverse	5´ TCGCTTTGGTCACTTTGTCTC 3´
PDE10A 115bp	Forward	5´ GACTTGATTGGCATCCTTGAA 3´
	Reverse	5´ CCTGGTGTATTGCTACGGAAG 3´
PDE11A 87bp	Forward	5´ CCCAGGCGATAAATAAGGTTC 3´
	Reverse	5´ TGCCACAGAATGGAAGATACA 3´
PBGD 135bp	Forward	5´ ATGTCCGGTAACGGCGGC 3´
	Reverse	5´ CAAGGTTTTCAGCATCGCTAC 3´

Table 5: Primer sequences for standard PCR

Gene (rat)		Primer Sequence
α **SMA 525bp**	Forward	5′ CGATAGAACACGGCATCATC 3′
	Reverse	5′ CATCAGGCAGTTCGTAGCTC 3′
Calponin 552bp	Forward	5′ GGGTGAAACCCCACGACATT 3′
	Reverse	5′ CGTCCAGCTCTGGATATTCC 3′
SM-MHC 529bp	Forward	5′ GCCAGAACAAGGAACTCCGA 3′
	Reverse	5′ GTTCCATTGAAGTCTGAGTCCC 3′
GAPDH 121bp	Forward	5′ GTCACCAGGGCTGCCTTCT 3′
	Reverse	5′ CATTGAACTTGCCGTGGGTA 3′

3.1. 6 Equipments

Equipment	**Company**
BioDoc Analyzer	Biometra, USA
Cell culture incubator, Hera Cell	Heraeus, Germany
Electrophoresis chamber	Biometra, USA
Fluorescence microscope	Leica, Germany
Freezer (+4˚C, -20 ˚C, -80 ˚C)	Bosch, Germany
Infinite® 200 microplate reader	Tecan, Switzerland
Inolab PH meter	WTW, Germany
Light microscope	Hund, Germany
Liquid scintillation counter, LS 6500	Beckmann, USA
Multifuge centrifuge	Heraeus, Germany
Mx3000P® QPCR system machine	Stratagene, USA
Spectrophotometer	NanoDrop Technologies, USA
PCR-thermocycler	Biometra, Germany
Pipetboy and pipettes	Eppendorf, USA
Power supply	Biometra, USA
Precellys®24 homogenizer	Bertin Technologies, France
Shaker	Biometra, USA
Water bath for cell culture	Medingen, Germany
Water bath for tubes	HLC, Germany
Western blot unit	Biometra, USA
Vortex machine	VWR, Germany

3.1. 7 Other materials

Falcon tubes, PCR tubes, glass pipettes and cell culture dishes and plates were purchased from Greiner Bio-One (Germany). Others are as listed below.

Material	Company
96-well microplate	Corning, USA
AGFA cronex 5 medical X-ray film	AGFA, Belgium
Chromatography column	Bio-Rad, USA
Film casette	Kodak, USA
Filter tips (10, 100, 1000µl)	Nerbe plus, Germany
Gel blotting paper	Whatman, USA
Nitrocellulose membrane	Pall Corparation, USA
Osmotic minipump (2 mL)	Durect Corparation, USA
Precellys bead mill sample tube	Bertin Technologies, France
Radiographic film hypersensitive	Amersham, USA
Santilation tube	Nerbe plus, Germany
Tips (10, 100, 1000µl)	Eppendorf, USA
Reaction tube	Sarstedt, Germany
Real time tube	Thermo Fisher, USA
Tissue culture chamber slide	BD Falcon, USA

3.2 Methods

3.2.1 Animals

Adult male Sprague-Dawley rats (250-300 g in body weight) were purchased from Charles River Laboratories (Sulzfeld, Germany). The experiments were performed in accordance with the National Institutes of Health Guidelines on the Use of Laboratory Animals. Both the University Animal Care Committee and the Federal Authorities for Animal Research of the Regierungspräsidium Giessen (Hessen, Germany) approved the study protocols.

3.2.1.1 Monocrotaline-induced pulmonary hypertensive rat model

Alkaloid monocrotaline was dissolved in 1 mol/L HCl and then adjusted to pH 7.4 with 1 mol/L NaOH, resulting in a clear solution with a final concentration of 20 mg/ml[58]. Rats were randomized for a one-shot subcutaneous (s.c.) injection of 60 mg/kg MCT to induce pulmonary hypertension, or an injection of the same

volume of saline to be as a control. Drinking water supplemented with antibiotic Baytril was given to MCT-injected rats for 2 weeks at the second day of MCT injection. Both of the control and MCT rats were kept up to 4 weeks for cell isolation, while for *in vivo* experiments rats were subjected to hemodynamic studies after 5 week of MCT injection.

3.2.1.2 Experimental groups

The animals were classified into the following three groups: 1) rats injected with saline and sacrificed after 35 days (Control, n=9); 2) MCT-injected rats subjected to minipump implantation from day 21 to day 35 with saline (MCT[35d]/saline, n=8); 3) MCT-injected rats subjected to minipump implantation from day 21 to day 35 with 5 mg/ml papaverine (MCT[35d]/papaverine, n=8).

3.2.1.3 Surgical preparation and hemodynamic measurements

Three weeks after MCT injection, rats were subjected to papaverine treatment for 2 weeks by implantation of osmotic minipumps (Alzet Model 2 mL). At day 21, after the rat was anaesthetized with an intraperitoneal injection (i.p.) of ketamine (9 mg/kg body mass) and medetomidine (100 µg/kg body mass), a minipump filled with 2 ml saline or with 2 ml papaverine (5 mg/ml) was implanted in the dorsal subcutaneous region under sterile conditions and a tunneled catheter (PE 50 tubing) was inserted into the left jugular vein. The releasing rate of the minipump is 5 µl per hour. After wound-closing with sutures, the rats were recovered from anesthesia by an intraperitoneal injection of naloxon and atipazemol (50 and 100 µg/kg body mass). At the end of the treatment, the rats were anesthetized with an intraperitoneal injection (*i.p.*) of ketamine (9 mg/kg body mass) and medetomidine (100 µg/kg body mass), followed by an intramuscular (*i.m.*) injection of heparin (50 IU/kg body mass) to measure the hemodynamic parameters. The rats were then tracheotomized and ventilated at a frequency of 60 breaths/min, with a positive end expiratory pressure at 1 cm H_2O throughout. To measure right ventricular pressure, a right heart catheter (PE 50 tube) was inserted through the right jugular vein and to measure arterial pressure a polyethylene catheter was inserted into the left carotid artery[84].

3.2.1.4 Histological assessment of the degree of muscularization of small pulmonary arteries

Three µm lung sections from blocks fixed in 3% paraformaldehyde solution were applied to a double staining with the anti-von Willebrand-factor antibody (1:900) and anti α-SMA antibody (1:900) for the analysis of small peripheral pulmonary artery muscularization. In each rat, 80 to 100 intraacinar arteries (20-50 µm) were categorized by the software as full muscularized, partially muscularized, or nonmuscularized, as previously described[84].

3.2.1.5 Tissue preparation

After the hemodynamic measurement, the lungs were flushed with saline via the pulmonary artery, the left lobes were snap frozen in liquid nitrogen and stored at -80°C for molecular studies while the right lobes were fixed in 3% paraformaldehyde solution for histological studies. Lungs for pulmonary artery isolation were freshly dissected and immersed in ice-cold Hank's balanced salt solution (HBSS) containing penicillin/streptomycin (P/S, 100 units/ml).

3.2.2 Isolation of pulmonary arterial smooth muscle cells (PASMCs)

Rat PASMCs were cultured from peripheral small pulmonary artery explants as previously described[85]. To isolate PASMCs, the freshly dissected rat lung was removed of lung parenchyma and interstitial tissues around the arteries until the small pulmonary arteries were completely exposed under a dissecting microscope. Then the adventitia layer was removed by micro-dissection. Artery segments were cut open along the longitudinal axis and the endothelium was gently removed by scraping the luminal surface. The arteries were minced into 1 mm^2 explant pieces and maintained in Dulbecco's modified Eagle's medium/F12 (DMEM/F12) supplemented with 10% fetal bovine serum (FBS), P/S (100 units/ml) and 2 mM L-glutamine. After 5 days PASMCs started to migrate from the explants, followed by 10 days of culturing. The morphology of PASMCs was observed under contrast microscopy and the early passages (passage 2-5) were used for all experiments. Every experiment in the following was performed with primary PASMCs isolated from at least 3 individual rats.

3.2.3 RNA interference

Transient transfection of siRNA was performed with X-tremeGENE siRNA transfection reagent according to the manufacturer's protocols. PASMCs were subcultured to 40% confluence in antibiotic-free DMEM supplemented with 10% FBS and 2 mM L-glutamine. siRNA and transfection reagent were diluted in opti-MEM and mixed within 5 min after dilution at a final ratio of 4:1 (transfection reagent µl to siRNA µg). After incubation for 20 min at RT, transfection of 100 nM siRNA was performed in opti-MEM for 5 h, followed by culturing in DMEM supplemented with 10% FBS and 2 mM L-glutamine up to 24 h (for RNA isolation) or 48 h (for protein isolation, enzyme immunoassay and proliferation assay). The RNA interference was well established and repeated at least three times.

3.2.4 Polymerase chain reaction (PCR)

3.2.4.1 RNA isolation

Total RNA from tissues or cells was extracted using Trizol according to the manufacturer's instructions. 50 mg lung tissue was applied to 1 ml Trizol and homogenized by Precellys24 homogenizer, or 2×10^6 PASMCs were collected in 1 ml Trizol. Trizol lysates were kept at RT for 5 min to dissociate the RNA from histone proteins. Then add 0.2 ml chloroform, vigorously mix for 15 sec and centrifuge under 12000 rpm at 4°C for 30 min. After that, the transparent upper layer was carefully transferred to a new tube and gently mixed with 0.5 ml 2-propanol. After 15 min the mixture was centrifuged under 12000 rpm at 4°C for 15 min and the RNA pellet was washed with 1 ml 75% ethanol and dried in the air. RNA was dissolved in DEPC-water and stored at -80°C. The concentration and quality of RNA were estimated by NanoDrop spectrophotometer.

3.2.4.2 Reverse transcription-PCR (RT-PCR)

cDNA was synthesized by a two-step RT-PCR using ImProm-II™ reverse transcription system according to the manufacturer's instructions. 1 µg RNA in 5 µl reaction A was denatured at 70°C for 5 min, followed by a quick chill for 5 min and addition of 15 µl reaction B. The reverse transcription reactions were

subjected to cDNA synthesis by firstly annealing at 25°C for 5 min and incubating at 42°C for 60 min, followed by thermal inactivation of reverse transcriptase at 70°C for 15 min. The cDNA was stored at -20°C.

Reaction A component	**Volume**	**Final concentration**
Total RNA, 1µg/ul	1 µl	1 µg/20µl
Oligo(dT)$_{15}$ primer, 0.5 µg/µl	1 µl	1 µg/20µl

Reaction B component	**Volume**	**Final concentration**
ImProm-II™ 5X reaction buffer	4 µl	1 X
$MgCl_2$, 25 mM	2 µl	2.5 mM
dNTP mix, 40 mM	1 µl	2 mM
RNasin® ribonuclease inhibitor	1 µl	20 u/20µl
ImProm-II™ reverse transcriptase	1 ul	0.5 u/20µl
Nuclease-free water to a final volume	15 µl	

3.2.4.3 Standard PCR

cDNA GoTaq® PCR core system I was applied for standard PCR using the program as follows. The annealing temperature is 58°C for GAPDH, αSMA (α-smooth muscle actin), SM-MHC (smooth muscle-myosin heavy chain) and Calponin. PCR reaction mixture was made as listed.

PCR reaction component	**Volume**	**Final concentration**
cDNA	2 µl	0.5 µg/25µl
$MgCl_2$, 25mM	2 µl	2 mM
dNTP mix, 40mM	0.5 µl	200 µM
Upstream primer, 10 µM	0.75 µl	0.3 µM
Downstream primer, 10 µM	0.75 µl	0.3 µM
5X Green GoTaq® flexi buffer	5 µl	1.0 X
GoTaq® DNA polymerase	0.25 µl	1.25 u/25µl
Nuclease-free water to a final volume	25 µl	

PCR programm	Temperature	Time	Cycle
Initial denaturation	95°C	2 min	1
Denaturation	95°C	1 min	
Annealing	Variable	1 min	30
Extension	72°C	1 min/kb	
Final extension	72°C	5 min	1
Soak	4°C	indefinite	1

3.2.4.4 Quantitative realtime- PCR (qRT-PCR)

The intron-spanning primer pairs were designed using the Primer3 program and are shown in Table 3. Primers were cross checked to insure the specificity by blasting to the whole genome. The product size is controlled within the range of 80 bp-150 bp.

qRT-PCR reaction component	Volume	Final concentration
cDNA	2 µl	0.2 µg/25µl
$MgCl_2$, 25 mM	1 µl	1 mM
ROX, 25 µM	0.1 µl	100 µM
Upstream primer, 10 µM	0.5 µl	0.2 µM
Downstream primer, 10 µM	0.5 µl	0.2 µM
2X SYBR® GreenER™ SuperMix Universal buffer	12.5 µl	1.0 X
Nuclease-free water to a final volume	25 µl	

qRT-PCR was performed on a Mx3000P® QPCR system machine using SYBR® GreenER™ qPCR SuperMixes Universal kits according to manufacturer's instructions. For the negative control, the cDNA was omitted. The annealing temperature for every gene is 58°C. By using the MxPro™ QPCR software, a dissociation curve was generated for each gene to ensure a single product amplification and the threshold cycle (Ct values) for each gene was determined. The comparative $2^{-\Delta\Delta Ct}$ method was used to analysis mRNA fold changes between control and MCT, which was calculated as Ratio = $2^{-(\Delta Ct}$

$^{control-\Delta Ct\ MCT)}$ where Ct is the cycle threshold, and ΔCt ($Ct_{target} - Ct_{reference}$) is the Ct value normalized to the reference gene Porphobilinogen Deaminase (PBGD) obtained for the same cDNA sample. Each reaction was run in duplicate and repeated three times independently. The calculated $2^{-\Delta\Delta Ct}$ was transformed into a percentage using the control as 100% to show the mRNA expression difference.

qRT-PCR programm	Temperature	Time	Cycle
Activation	95°C	10 min	1
Denaturation	95°C	30 sec	40
Annealing	58°C	30 sec	
Extension	72°C	30 sec	
Denaturating	95°C	1 min	
Dissociation curve	55-95°C	indefinite	1
Soak	4°C	indefinite	1

3.2.4.5 Agarose gel electrophoresis of DNA

PCR products together with DNA ladder (100bp, 1kb) were loaded on 1.5% agarose gel containing 1 µg/ml ethidium bromide and were run in tris-acetate-EDTA (TAE) buffer at 100 V until separated. The DNA bands were detect by UV illumination and captured by BioDoc Analyzer.

TAE buffer component	Final concentration
Tris-HCl	40 mM
Acetic acid	40 mM
EDTA , 0.5 M, pH 8.0	1 mM

3.2.5 Western blotting

3.2.5.1 Protein isolation

Total protein was extracted in RIPA buffer containing 1XTBS, 1% Nonidet P-40, 0.5% sodium deoxycholate, 0.1% SDS, 0.004% sodium azide. PMSF, proteinase inhibitor cocktail and sodium orthovanadate (10µl each in 1 ml RIPA) were added to RIPA freshly before use. 100 mg lung tissue homogenized in 800 µl RIPA or 2×10^6 PASMCs in 250 µl RIPA was centrifuged under 12000 rpm for 30 min at 4°C and the supernatants were stored at -80°C.

3.2.5.2 Protein concentration analysis

A series of bovine serum albumin (BSA) solution from 0.2-1.6 mg/ml were used as standard. The protein samples were pre-diluted into the range of the standard and the concentration of each sample was double estimated by D_c protein assay kit based on the method of Bradford using a microplate reader.

3.2.5.3 SDS-polyacrylamide (SDS-PAGE) gel electrophoresis

Protein samples of the same concentration were mixed with 5× SDS gel-loading buffer at a ratio of 4:1 (v/v) and denatured at 100°C for 5 min. Protein samples (30 µg for PDE10A, CREB and pCREB; 15 ug for GAPDH) or rainbow marker were loaded in the wells of 10% SDS-PAGE gel and run at 100-130 v for 2-3 hours to separate. Buffers are listed as follows.

5×SDS gel-loading buffer component	Final concentration
Tris-Cl (2 M, pH 6.8)	375 mM
SDS	10% (w/v)
Glycerol	50% (v/v)
β-Mercaptoethanol	12.5% (v/v)
Bromophenol blue	0.02% (w/v)

Running buffer component	Final concentration
Tris-HCl	25 mM
Glycine	192 mM
SDS 10% (w/v)	0.1% (w/v)

Resolving gel (10%) component	Volume	Final concentration
Tris-Cl (1.5 M, pH 8.8)	0.625 ml	375 mM
Acrylamid 30% (w/v)	0.5 ml	10% (w/v)
SDS 10% (w/v)	25 µl	0.1% (w/v)
APS 10% (w/v)	12.5 µl	0.05% (w/v)

Stacking gel (6%) component	Volume	Final concentration
Tris-Cl (0.5 M, pH 6.8)	1.5 ml	375 mM
Acrylamid 30% (w/v)	2 ml	10% (w/v)
SDS 10% (w/v)	60 µl	0.1% (w/v)
APS 10% (w/v)	30 µl	0.05% (w/v)
TEMED	6 µl	0.1%
H_2O	2.4 ml	

3.2.5.4 Immunoblotting

The proteins separated on the SDS-PAGE were transferred to nitrocellulose membrane using an electrophoretic transfer machine. After being soaked in blocking buffer for 1 h at RT, membranes were probed with specific primary antibodies (rabbit polyclonal anti-PDE10A antibody,1:2000; rabbit polyclonal anti-CREB antibody, 1:000; rabbit polyclonal anti-phospho-CREB(Ser133) antibody, 1:000; mouse monoclonal anti-GAPDH antibody, 1:5000) overnight at 4°C. After wash with TBST for 3 times, horse radish peroxidase (HRP)-conjugated secondary antibodies (anti-rabbit, 1:50000; anti-mouse, 1:50000) were applied to the membranes respectively for 1 h at RT. After washing, the blots were developed with an enhanced chemiluminescence (ECL) kit for 5 min and chemiluminescence signal was captured on an X-ray film. Each blot was repeated twice independently with representative blots shown.

Blotting buffer	Final concentration
Tris-HCl	50 mM
Glycine	40 mM
Methanol	20% (v/v)

TBST buffer (pH 7.6) component	Final concentration
Tris-HCl	20 mM
NaCl	137 mM
Tween	0.1% (v/v)
Blocking buffer component	**Final concentration**
Non-fat milk	5% (w/v) in TBST

3.2.6 Immunohistochemistry

Three μm lung sections were cut from lung blocks fixed in 3% paraformaldehyde solution. After deparaffinization in xylene and rehydration in a series of grade-decreasing ethanol solutions followed by phosphate-buffered saline (PBS), the antigen retrieval was achieved by 0.25% trypsin for 15min at 37°C. Then a NovaRED horseradish peroxidase (HRP)-substrate kit was applied for immunohistochemistry staining according to the manufacturer's instructions. After being treated with 3% hydrogen peroxide for 20 min to block the endogenous peroxidases and serum blocking for 1 h, the sections were subjected to anti-PDE10A polyclonal antibody (1:200, in 10% BSA) overnight at 4°C. After washing, the corresponding secondary antibody conjugated with HRP was applied for 30 min. After washing, color development was carried out with a substrate/chromogen mixture, followed by counterstaining with hematoxylin. The sections were examined under a Leica DM 2500 microscopy using Leica QWin imaging software. Sections from 4 rats of each group were stained with the representative staining shown. The sections without secondary antibodies were negative controls.

3.2.7 Immunocytochemistry

Rat PASMCs grown on 8-well chamber slides were fixed with the ice-chilled acetone-methanol mixture (1:1) for 10 min at 4°C. After washing with PBS, the fixed cells were sequentially incubated with blocking buffer (3% BSA in PBS） for 1 h at RT, and then the primary antibody against αSMA (1:1000 in blocking buffer) for 1 h at RT or against PDE10A (1:200 in blocking buffer) overnight at 4°C. After the primary antibodies, cells were washed 5 times with PBS and

subjected to FITC-conjugated anti-mouse or Alexa Fluor® 488 anti-rabbit secondary antibody (1:1000 in blocking buffer) for 1 h at RT in dark. Then cells were washed 5 times with PBS and counterstained for nuclei with DAPI (500 ng/ml in blocking buffer) for 3 min. After washing with PBS, the upper chamber was removed and the slide was covered with a cover slide using the fluorescent mounting medium. The staining was visualized using a Leica DMLA fluorescence microscope and Leica QWin imaging software. PASMCs from 3 individual rats of each group were stained with the representative staining shown. The wells without primary antibodies were negative controls.

3.2.8 PDE inhibitors

3-Isobutyl-1-methylxanthine (IBMX) was used as a nonspecific PDE inhibitor. 8-Methoxymethyl-IBMX (8MM-IBMX), erythro-9-(2-Hydroxy-3-nonyl) adenine (EHNA), milrinone, rolipram, sildenafil and papaverine were used as relatively selective PDE inhibitors for PDE1, PDE2, PDE3, PDE4, PDE5 and PDE10 respectively.

3.2.9 PDE activity assay

cAMP specific PDE activities were determined by a modified method of Thompson and Appleman and Bauer and Schwabe[86, 87]. The PASMC protein was extracted by RIPA buffer and equalized to the same concentration for use. The reactions were performed with 10 µg protein in 100 µl reaction buffer at 37°C for 15 min. Then the samples were boiled for 3 min, subsequently cooled for 5 min and incubated with 25 µl Crotalus atrox snake venom (20 mg/ml) for 15 min at 37°C. After being chilled on ice, the samples were applied to QAE Sephadex A-25 mini-chromatography columns and eluted with 1ml ammonium formate (30 mM, pH 7.5). The elutes were collected in 2 ml scintillation solution and counted by a beta-counter giving a CPM (counts per minute) value. Data were expressed as picomoles of cAMP per minute per milligram of protein (pmol cAMP / minute / mg protein). Each assay was performed in triplicate and repeated twice independently.

PDE activity reaction buffer	Final concentration
HEPES (1 M, pH 7.6)	40 mM
$MgCl_2$	5 mM
BSA	1 mg/ml
cAMP	1 μM
[^{3}H]-cAMP (1 mCi/ml)	1 μCi/ml

3.2.10 cAMP enzyme immunoassay (EIA)

Intracellular cAMP content of PASMCs was determined by a competitive non-acetylated EIA, using a specific cAMP EIA Kit according to the manufacturer's instructions. At the end of culture, cells were washed twice with PBS and lysed in 0.1 M HCl at RT for 20 min. The lysates were collected and centrifuged under 12000 rpm for 30min at 4°C. The supernatant was transferred to a new tube and stored at -80°C. The protein concentration was estimated by the D_c protein assay as described before and equalized to 0.3 μg/μl for use. 50 μl protein samples or standard solutions were incubated in dark with 50 μl tracer and 50 μl antibody overnight at 4°C. After washing 5 times, the plate was incubated with Ellman's solution for 90-120 min at RT with gentle shaking. The plate was read at a wavelength of 405 nm and the concentration was calculated by the ready-made Cayman EIA Double workbook. The standard curve was made as a plot of the $\%B/B_0$ value (%Bound/Maximum Bound) *vs* concentration of a series of known standards using a linear (y) and a log (x) axis. Using the 4-parameter logistic equation obtained from the standard curve, the cAMP concentration of samples was determined and given as nmol/mg protein. Each sample was performed in duplicate and repeated twice.

3.2.11 Proliferation assay

PASMC proliferation was achieved by [^{3}H]-thymidine incorporation assay as described previously[58]. PASMCs (around 1×10^4 cells/well) were seed on 48-well plates and the following day the medium was substituted with DMEM/F12 containing 0.1% FBS with or without siRNA to render the cells quiescent. After 24-h serum starvation, cells were induced to cell cycle reentry by 10% FBS

together with different PDE inhibitors for 24 h. The concentration of PDE inhibitors used for proliferation assay was pre-proved for PDE selectivity according to the previous reports[83, 88]. During the last 4 h of FBS stimulation, 10 µl [^{3}H]-thymidine (0.01 µCi/ml) was added to 250 µl medium to incorporate into the DNA. Cells were then washed twice with 500 µl chilled HBSS, fixed with 250 µl ice-cold methanol for 15 min at 4°C and then precipitated by 250 µl 10% trichloroacetic acid (TCA) for 15 min at 4°C. After washing with water, samples were finally lysed in 0.1 M NaOH, transferred into 4 ml scintillation solution and counted by a beta counter giving a CPM value. All labeling was performed on quadruplicate cultures and repeated twice independently. The proliferation of PASMCs under 10% FBS stimulation is shown as a percentage taking the CPM of unstimulated PASMCs under 0.1% FBS as 100%.

3.2.12 Statistical analysis

Data are expressed as mean and standard error of mean (SEM). All statistical analysis was performed with Student's *t*-test between two groups or with one-way ANOVA and Newman-Keuls post-hoc test for multiple comparisions, as appropriate. Difference between groups is considered significant when $P < 0.05$.

4 RESULTS

4.1 Primary PASMCs isolation and characterization

Small pulmonary arteries (Figure 8A, in white squares) dissected from the rat lung were subjected to PASMC isolation. Primary PASMCs in early passages exhibited typical spindle-shape morphology and grew with a “hill-and-valley” pattern (Figure 8B). To ensure the property and purity of isolated PASMCs, the presence of key vascular smooth muscle cell markers were assessed by semi-quantitative PCR or by immunocytochemistry. Vascular SMC phenotype genes including αSMA, SM-MHC and calponin are all equally expressed in cells isolated from control and MCT-PH rats on mRNA level (Figure 8C), which is confirmed by a 98% positive staining in cells against αSMA (Figure 8D).

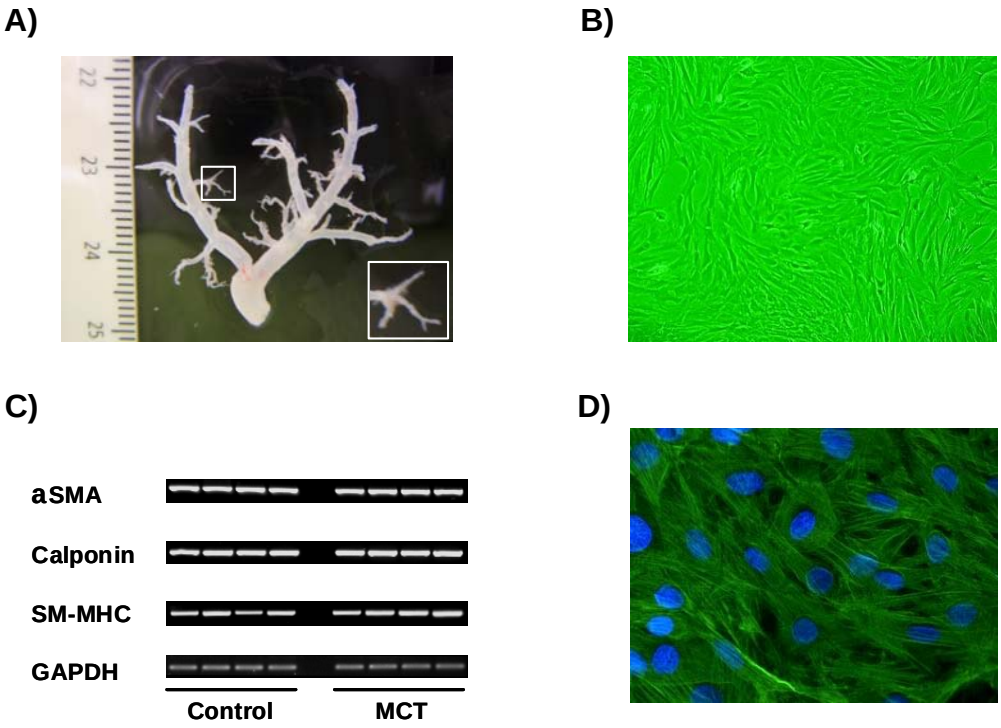

Figure 8: Primary PASMCs cultured from small pulmonary arteries. A) Pulmonary artery branches freshly dissected from a rat lung. The small artery (less than 0.5 mm in diameter) in the white square magnified in the right corner was used for PASMC isolation. **B)** Morphology of rat PASMCs with a 90% confluence at passage 1 observed by a phase-contrast microscope. **C)** mRNA expression of vascular SMC phenotypic genes in both control and MCT PASMCs by semi-quantitive PCR. **D)** Immunocytochemistry staining of isolated cells against αSMA. PASMCs showed a positive staining of αSMA fibers in green with nucleus stained blue by DAPI.

4.2 Profiling of PDE7-11 expression in rat lungs and PASMCs

4.2.1 Expression of PDE711 isoforms in rat lung tissue

Expression of newly identified PDEs (PDE7-11) in lungs from both control rats and MCT-PH rats was investigated by qRT-PCR. In rat lung tissue, PDE7-11 isoforms were all expressed on mRNA level. Out of those PDEs, PDE7A, PDE7B and PDE10A were significantly upregulated (264.7±16.2%, 230.7±25.3% and 140.6±9.5% of control respectively), while PDE8B was downregulated (50.2±6.9% of control) in MCT-PH lungs as compared to control lungs. PDE8A, PDE9A and PDE11A were shown on the same level in both groups (Figure 9).

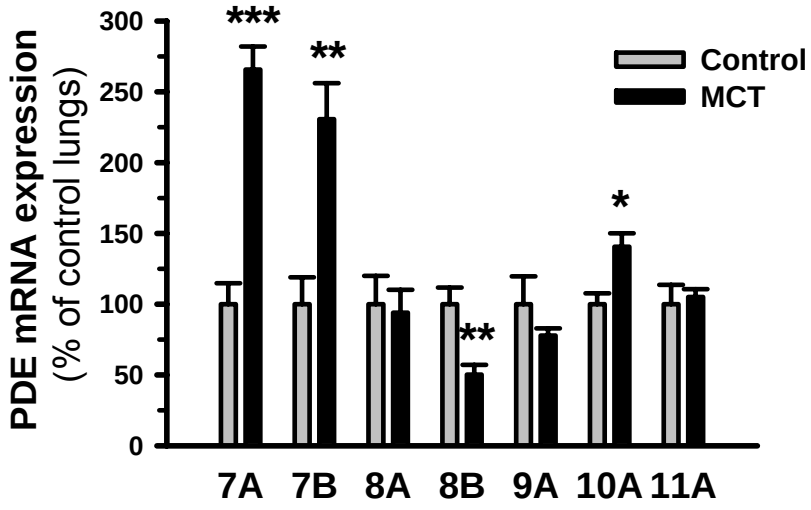

Figure 9: mRNA expression of PDE7-11 isoforms in rat lung tissue. Relative mRNA levels of PDE7-11 in lung homogenates from control rats (grey bars) and from 4-week MCT rats (black bars) were shown as a percentage of control by qRT-PCR after normalization to PBGD. *P < 0.05, **P < 0.01, ***P < 0.001 *vs* control lungs. n = 4 in each group. Values are expressed as mean ± SEM.

4.2.2 Expression of PDE7-11 isoforms in rat PASMCs

In the isolated PASMCs, we discovered that only PDE7A, PDE7B, PDE8A, PDE10A and PDE11A are present, with an increase of PDE7A (259.4±11.1% of control) and PDE10A (254.9±36.9% of control) in MCT-PH PASMCs as compared to control PASMCs (Figure 10).

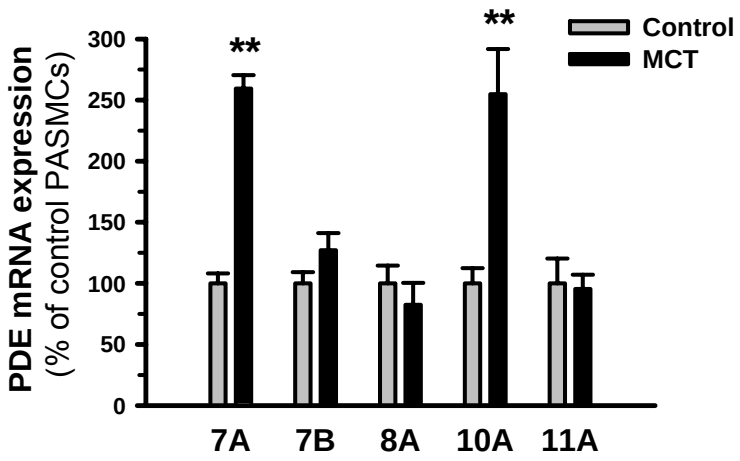

Figure 10: mRNA expression of PDE7-11 isoforms in rat PASMCs. Relative mRNA levels of PDE 7-11 in PASMCs from control rats (grey bars) and from 4-week MCT rats (black bars) were shown as percentage of control by qRT-PCR after normalization to PBGD. **P < 0.01 *vs* control PASMCs. n = 4 in each group. Values are expressed as mean ± SEM.

4.3 PDE10A localization and expression in pulmonary vasculature

4.3.1 PDE10A localization in rat lung

Since PDE10A was the first time described in the adult rat lung, immunohistochemistry was performed in lung sections to verify PDE10A expression pattern in rat lung. A stronger immunoreactivity of PDE10A was observed in lung specimens from MCT-PH rats, suggesting that the site-specific change of PDE10A occurred especially in the medial layer of the pulmonary arteries (Figure 11 c,d). In contrast, only weak expression of PDE10A was detected in pulmonary vessels of control rat lung (Figure 11 a,b). In addition, immunoreactivity against PDE10A was also noted in bronchial SMCs of the small airways.

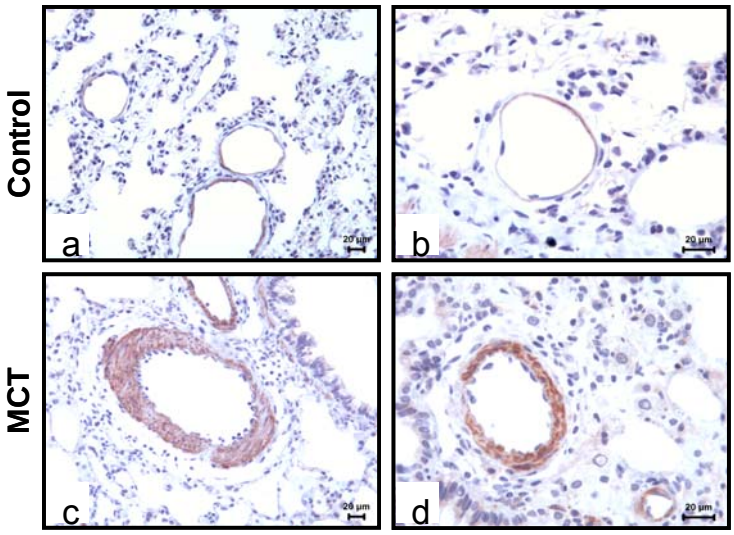

Figure 11: Immunohistochemistry staining of PDE10A in rat lung sections. Representative staining of lung sections from control rats (a,b) and MCT rats (c,d) shows dominant PDE10A expression in rat PASMCs. PA means pulmonary artery. Scale bar: 20 µm.

4.3.2 PDE10A expression is exclusively induced in pulmonary vasculature

To investigate whether if PDE10A induction is specific in remodeled pulmonary vasculature, we examined PDE10A expression in the pulmonary artery and in the systemic arteries including aortic artery and femoral artery. qRT-PCR data showed a 2-fold increase of PDE10A mRNA expression in the pulmonary artery of MCT-PH rats compared to control rats, with no changes in either the aortic artery or femoral artery (Figure 12).

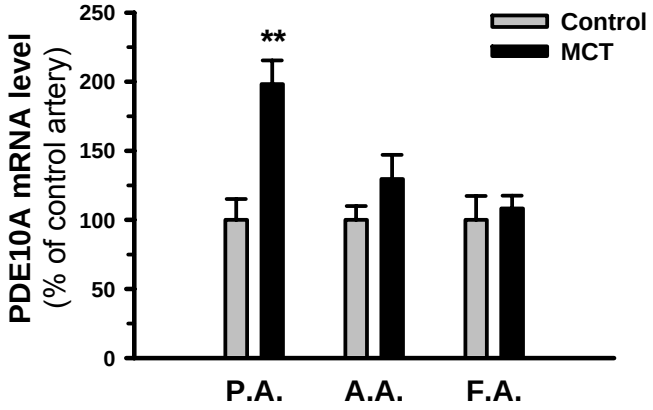

Figure 12: PDE10A mRNA expression in pulmonary and systemic vessels. qRT-PCR analysis of PDE10A expression in the pulmonary artery (P.A.), aortic artery (A.A.) and femoral artery (F.A.) from control rats (grey bars) and 4-week MCT rats (black bars), shown as a percentage of control after normalization to PBGD. **P < 0.01 *vs* control. n = 4 in each group. Values are expressed as mean ± SEM.

4.4 PDE10A expression, activity and localization in rat PASMCs

4.4.1 Protein expression of PDE10A in rat PASMCs

In corroboration of increased PDE10A expression on the immunoreactivity level and the mRNA level in pulmonary vessels, immunoblotting demonstrated a 1.6-fold increase of PDE10A in MCT-PH PASMCs compared to control PASMCs (Figure 13A and 13B).

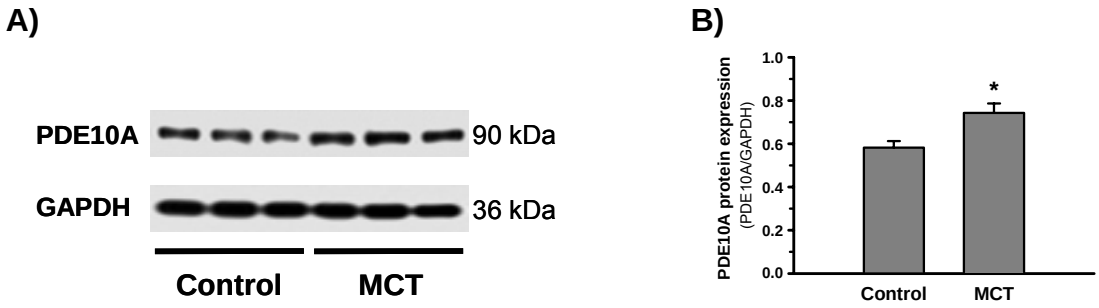

Figure 13: PDE10A protein expression in rat PASMCs. A) Representative immunoblots against PDE10A with GAPDH as a loading control. **B)** Densitometric quantification of PDE10A expression in PASMCs is shown as a ratio by normalization to GAPDH in a bar graph. *P < 0.05 *vs* control PASMCs. n = 3 in each group. Values are expressed as mean ± SEM.

4.4.2 Enzyme activity of PDE10A in PASMCs

To assess the enzymatic activity of PDE10A, cAMP hydrolyzing PDE activity assays were performed. PDE activity assay demonstrated higher total cAMP hydrolyzing activity in MCT-PH PASMCs than in control PASMCs (8.72 vs 7.66 pmol cAMP/minute/mg protein), which were both suppressed by IBMX to a similar basal level (1.9 pmol cAMP/minute/mg protein) (Figure 14A). Interestingly, the contribution of PDE10A to the total cAMP PDE activity increased from 38% to 53% in MCT-PH PASMCs as opposed to control PASMCs (Figure 14B and 14C). In contrast, the contribution of other cAMP hydrolyzing PDEs (PDE1, PDE2, PDE3 and PDE4) declined from 70% to 52% in MCT-PH PASMCs as compared to control PASMCs (Figure 14B and 14C).

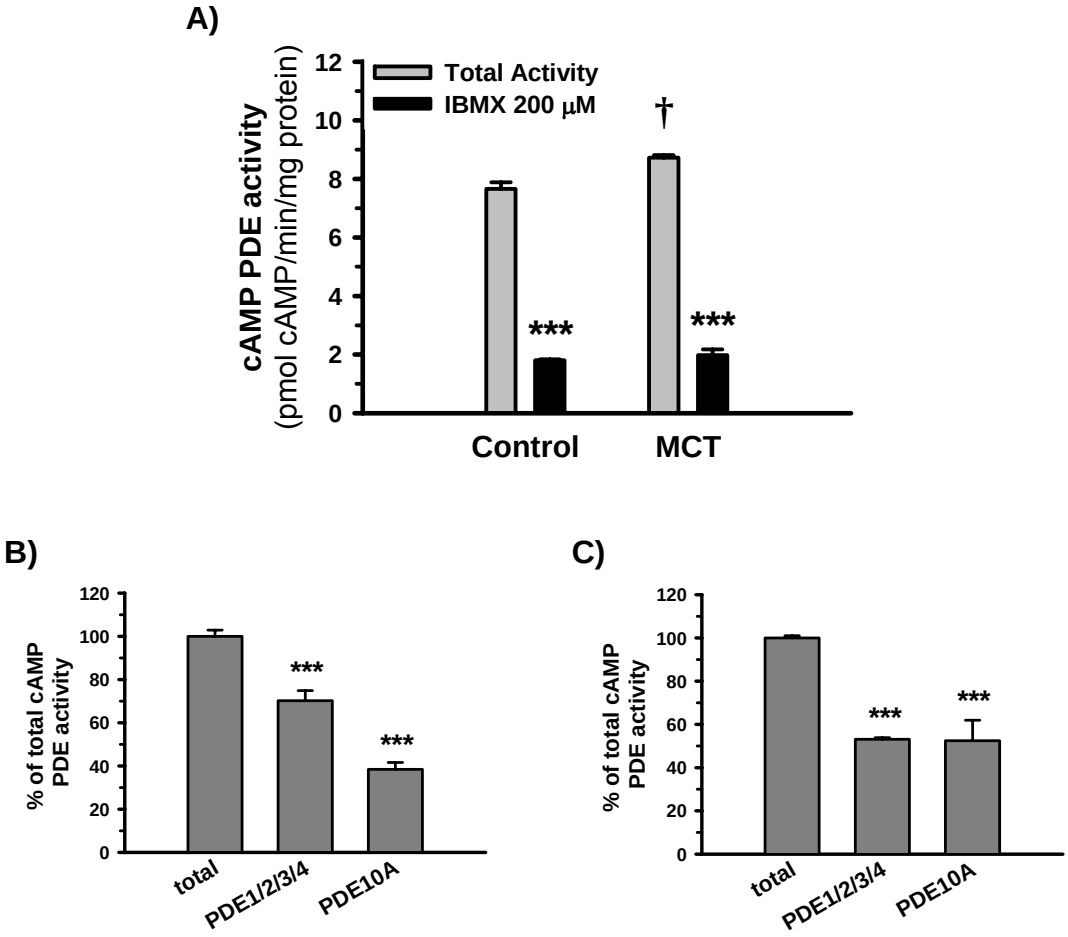

Figure 14: cAMP PDE activity of control and MCT PASMCs. PDE activity assay was performed by applying different PDE inhibitors to protein lysates of PASMCs. **A)** Total cAMP activity in control and in MCT PASMCs. The PDE activity in both was remarkably suppressed by a non-selective PDE inhibitor (IBMX, 200 µM) to a similar basal level (black bars). †P < 0.05 *vs* control PASMCs; ***P < 0.001 *vs* total activity. cAMP activity of **B)** control PASMCs and **C)** MCT PASMCs attributed by PDE10A or other PDEs (PDE1, PDE2, PDE3 and PDE4). Total cAMP PDE activity was suppressed in varying degrees by a PDE10A inhibitor (papaverine, 10 µM) or by a combination of inhibitors against PDE1 (8MM-IBMX, 30 µM), PDE2 (EHNA, 30 µM), PDE3 (milrinone, 5 µM) and PDE4 (rolipram, 10 µM). ***P < 0.001 *vs* total activity. n = 3 in each group. Values are expressed as mean ± SEM.

4.4.3 Cellular localization of PDE10A in rat PASMCs

Indicated by the high abundance of PDE10A in PASMCs by immunohistochemistry analysis of lung sections, we further investigated the cellular localization of PDE10A in PASMCs. Immunofluorescence staining showed a predominant presence of PDE10A in the nuclei of control PASMCs as well as MCT PASMCs (Figure 15).

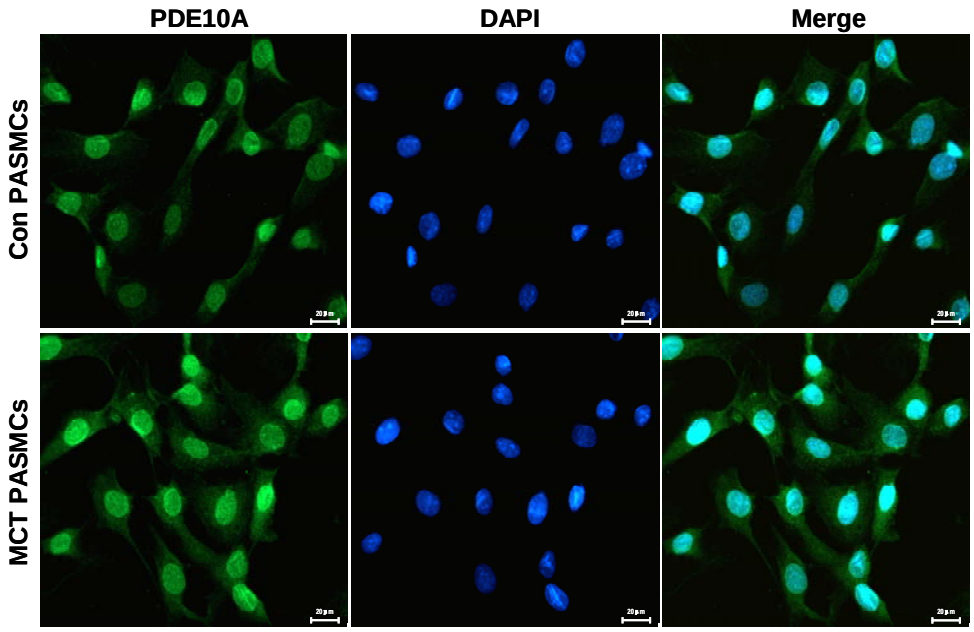

Figure 15: Immunocytochemical staining of PDE10A in PASMCs. Cellular localization of PDE10A in control PASMCs and MCT PASMCs, shown by representative immunofluorescence. Green (PDE10A, FITC-conjugated); Blue (nuclei, DAPI). Staining is shown in a 400×magnification.

4.5 Pulmonary hypersentive PASMCs are more proliferative than control PASMCs

To examine whether PASMCs from MCT-PH rats are more proliferative, we applied [^{3}H]-thymidine incorporation assay on both control and MCT-PH PASMCs under FBS stimulation. [^{3}H] uptake is 80% higher in MCT-PH PASMCs than in control PASMCs (Figure 16). Due to this pathophysiology relevant cell phenotype of PASMCs from MCT-PH rats as compared to control PASMCs, all further experiments delineating the contribution of PDE10A were performed in MCT PASMCs.

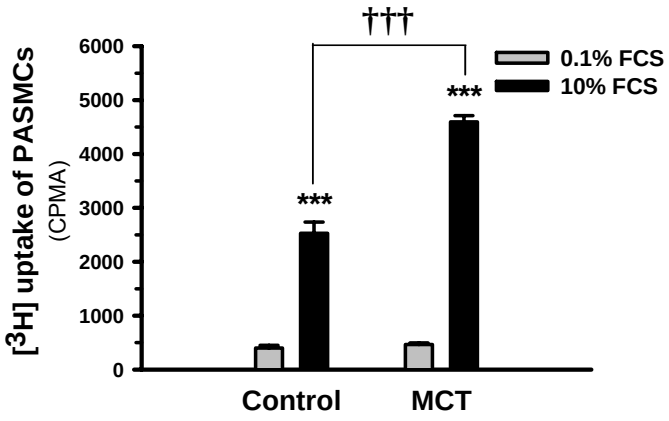

Figure 16: Cell proliferation of control and MCT PASMCs. Thymidine uptake of control and MCT PASMC under 10% FBS stimulation for 24-h. [^{3}H]-thymidine incorporation was

shown with CPMA. ***P < 0.001 *vs* 10% FBS; †††P < 0.001 *vs* control. n = 4 in each group. Values are expressed as mean ± SEM.

4.6 Pharmacological and genetic inhibition of PDE10A affects intracellular cAMP level and proliferation of PASMCs

4.6.1 Effects of PDE10A inhibitor papaverine on cAMP accumulation and PASMC proliferation

To investigate the functional role of PDE10A in MCT-PH PASMCs, we used the PDE10 inhibitor papaverine to block the endogenous PDE10A in PASMCs. EIA assay showed a basal intracellular cAMP level in MCT-PH PASMCs at 0.53±0.02 (nmol/mg protein). Papaverine (10 μM; 25 μM) dose-dependently elevated intracellular cAMP to 0.87±0.20 and 1.15±0.17 (nmol/mg protein) respectively (Figure 17A). The proliferation of PASMCs stimulated by 10% FBS was reduced to 60% by 25 μM papaverine, as assessed by [^{3}H]-thymidine incorporation assay (Figure 17B).

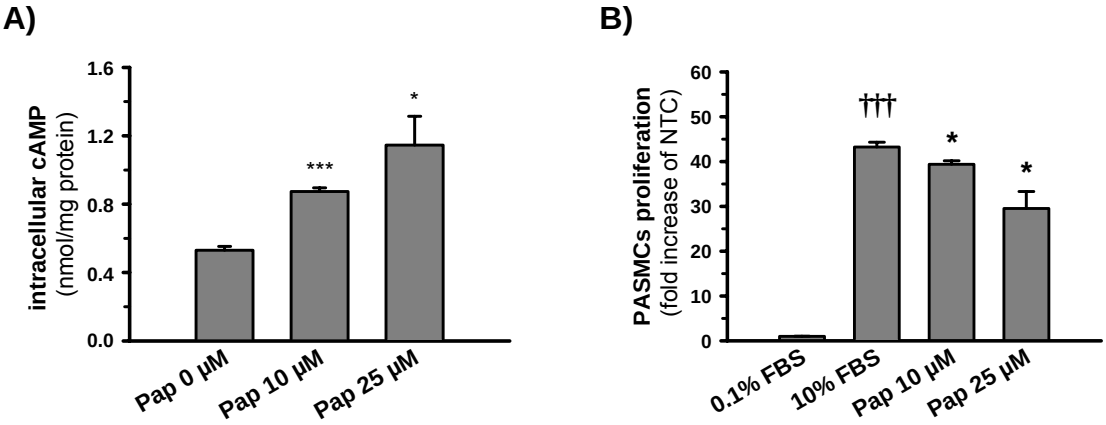

Figure 17: PDE10A inhibitor papaverine accumulates intracellular cAMP and attenuates PASMCs proliferation. A) Intracellular cAMP of PASMCs was remarkably increased after papaverine treatment. MCT PASMCs were treated with papaverine (0, 10, 25 μM) for 24 h for cAMP EIA assay. The cAMP content of PASMC lysates is given as nmol/mg protein. *P < 0.05; ***P < 0.001 *vs* papaverine untreated. n = 4 in each group. **B)** PASMC proliferation was reduced by papaverine. After serum starvation MCT PASMCs were stimulated by 10% FBS alone or with papaverine (10 μM, 25 μM) for 24 h. [^{3}H]-thymidine incorporation was used to evaluate cell proliferation. †††P < 0.001 *vs* 0.1% FBS; *P < 0.05 *vs* 10% FBS. n = 4 in each group. Values are expressed as mean ± SEM.

4.6.2 Effects of PDE10A knockdown by si-PDE10A on cAMP accumulation and PASMC proliferation

4.6.2.1 PDE10A knockdown by siRNA

In addition to the inhibitor studies, siRNA targeting PDE10A was applied to knockdown the endogenous PDE10A in MCT-PH PASMCs to be more specific with PDE10A inhibition. PDE10A was successfully suppressed by 100 nM si-PDE10A on the level of mRNA (25.2±0.4% of NTC) (Figure 18A), protein (Figure 18C) and activity (31.5±4.5% of NTC) (Figure 18D), while no changes accrued by 100nM scramble siRNA. In addition, to examine isoform-specific effects of si-PDE10A, the expression of other PDE isoforms was analyzed in the PASMCs treated with si-PDE10A or scramble siRNA. Results suggested that these effects were specific, and the PDE10A siRNA oligos had no effect on the expression of PDE1A, PDE3A and PDE3B isoforms (Figure 18B).

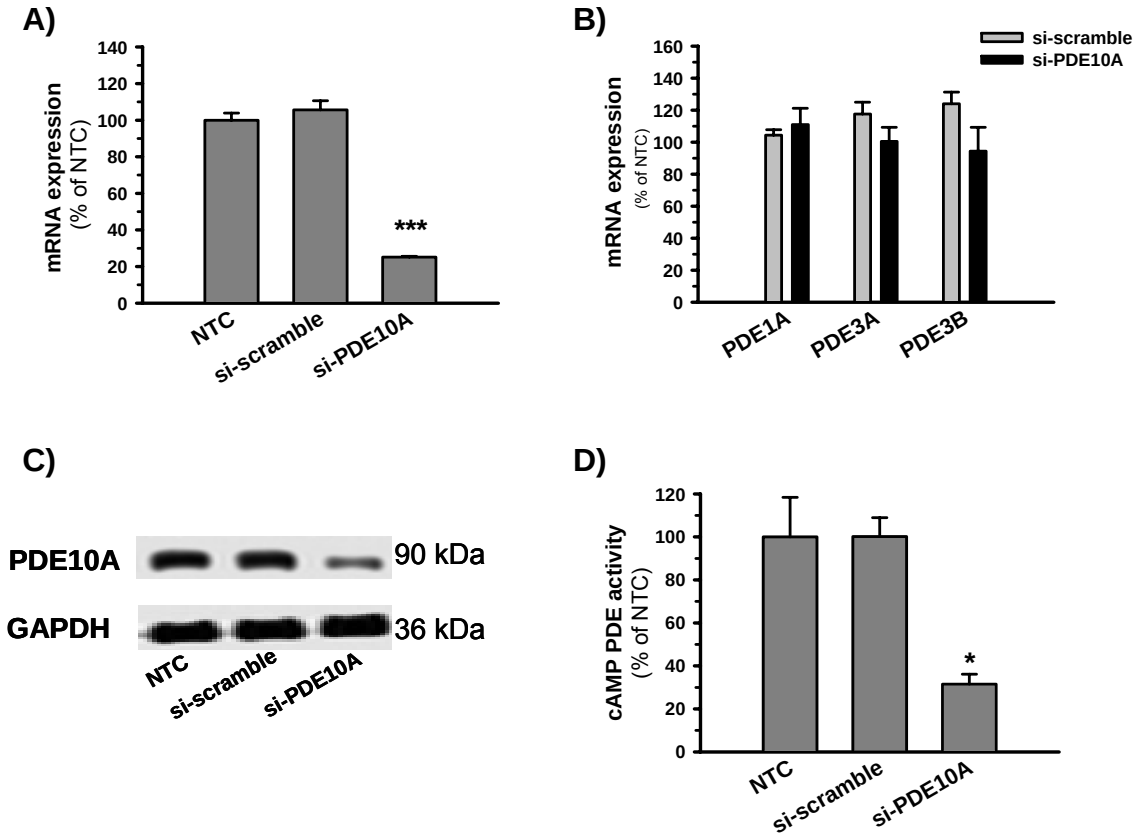

Figure 18: Knockdown of PDE10A by specific siRNA. MCT PASMCs were transiently transfected with 100 nM of si-scramble or si-PDE10A for 24 h or 48 h. PASMCs treated with transfection reagent alone is the negative control (NTC). **A)** PDE10A mRNA expression decreased after 24 h si-PDE10A transfection, as shown by qRT-PCR. ***P < 0.001 *vs* NTC. n = 3 in each group. **B)** PDE1A, PDE3A and PDE3B mRNA expression after 24 h transfection of 100 nM si-scramble (grey bars) or si-PDE10A (black bars). n = 3 in each group. **C)** Representative immumoblots showed suppressed PDE10A protein

expression in MCT PASMCs after 48 h si-PDE10A transfection. GAPDH was taken as a loading control. **D)** Total cAMP PDE activity in MCT PASMCs was dramatically reduced by 48 h si-PDE10A knockdown, as estimated by PDE activity assay. *P < 0.05 *vs* NTC. n = 4 in each group. Values are expressed as mean ± SEM.

4.6.2.2 Knockdown of PDE10A by siRNA accumulates intracellular cAMP and attenuates PASMC proliferation

With established siRNA knockdown conditions, the cAMP level of MCT-PH PASMCs was examined after PDE10A suppression by siRNA. Intracellular cAMP was increased to 1.00±0.10 (nmol/mg protein) in si-PDE10A treated PASMCs, compared with 0.48±0.04 (nmol/mg protein) in untreated PASMCs or 0.55±0.03 (nmol/mg protein) in scramble siRNA treated PASMCs (Figure 19A). 10% FBS stimulated proliferation of MCT-PH PASMCs was remarkably attenuated to 60% by si-PDE10A, without any changes with scramble siRNA (Figure 19B).

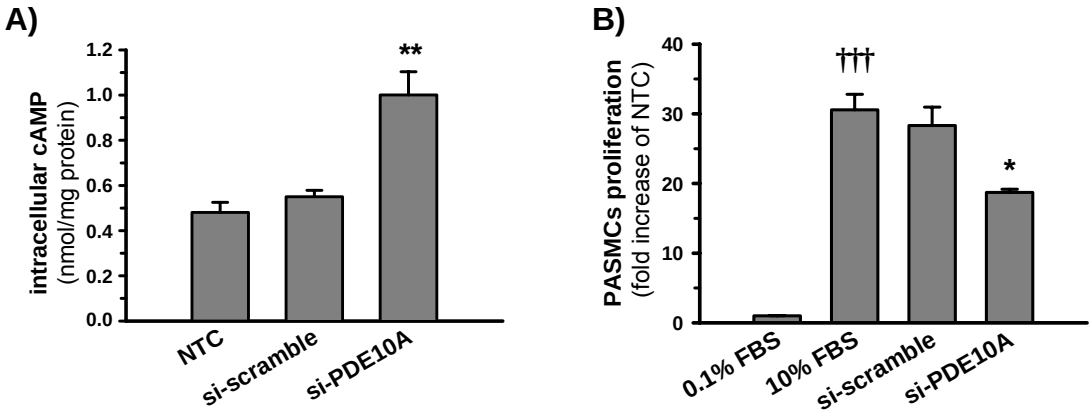

Figure 19: si-PDE10A accumulates intracellular cAMP and attenuates PASMC proliferation. A) Intracellular cAMP was increased in MCT PASMCs after PDE10A knockdown by siRNA for 48 h, evaluated by EIA assay. **P < 0.01 *vs* NTC. n = 4 in each group. **B)** PASMC proliferation was attenuated by 48 h PDE10A knockdown, as shown by [^{3}H]-thymidine incorporation assay. †††P < 0.001 *vs* 0.1% FBS; *P < 0.05 *vs* 10% FBS. n = 4 in each group. Values are expressed as mean ± SEM.

4.7 Inhibiton of PDE10A modulates CREB phosphorylation

cAMP response element binding protein (CREB) is an important downstream target of cAMP. We attempted to address if CREB is modulated by PDE10A inhibition. Immunoblots indicated CREB activation with increased phospho-CREB (Ser133) after “loss of function” of PDE10A using papaverine (10 µM; 25 µM) (Figure 20A) and si-PDE10A (100 nM) (Figure 20B).

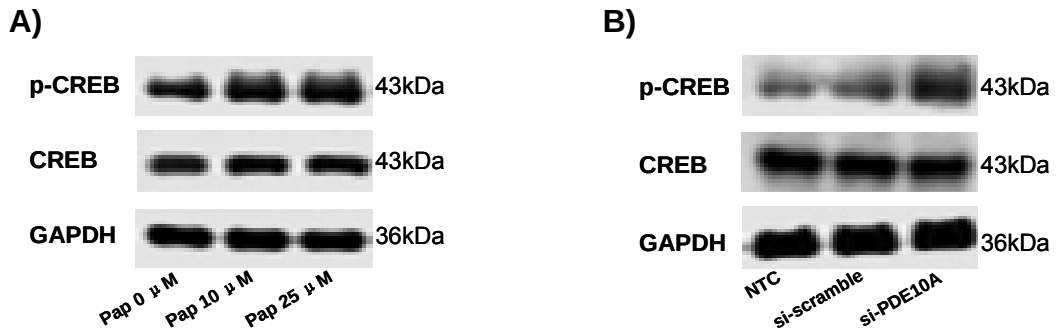

Figure 20: Activation of CREB by PDE10A inhibition. Protein from **A)** papaverine (24 h, 10 µM; 25 µM) or **B)** si-PDE10A (48 h, 100 nM) treated MCT PASMCs was applied for immunoblotting against phospho-CREB (ser133) and total CREB, with GAPDH as a loading control. Each blot was repeated twice.

4.8 Antiproliferative effects of PDE inhibitors on PASMCs.

Since cAMP and cGMP are key factors in the regulation of cell cycle and vasculature remodeling, we tested the contribution of different PDEs to the proliferation of MCT-PH PASMCs by using selective PDE inhibitors. IBMX (300 µM), as a universal PDE inhibitor, was used as a positive control and inhibited PASMC proliferation by 65%. PASMC proliferation was reduced similarly by ~ 25% either with PDE3 inhibitor (milrinone), PDE4 inhibitor (rolipram) or PDE5 inhibitor (sildenafil); while PDE10 inhibitor (papaverine) decreased PASMC proliferation by 40% (Figure 21), which is to a higher extent as compared to other PDE inhibitors. We concluded that among all these PDEs, PDE10 contributes the most to proliferation of pulmonary hypertensive PASMCs.

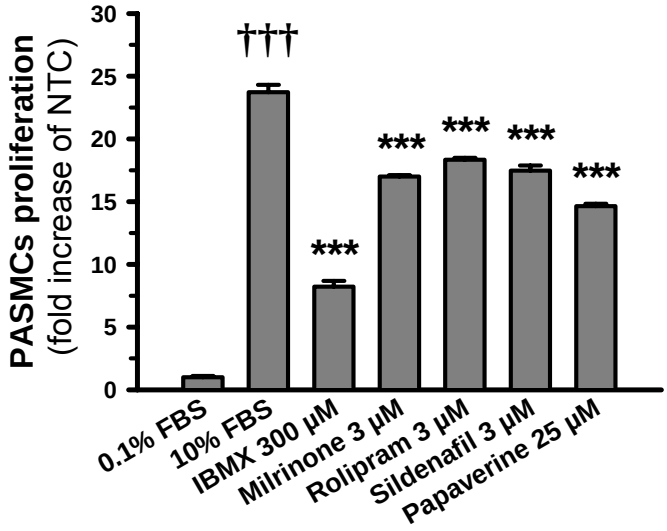

Figure 21: Anti-proliferative effect of isoform selective PDE inhibitors. MCT PASMCs underwent serum starvation and were subsequently stimulated to proliferate by 10% FBS.

PDE inhibitors (IBMX, 300 µM, universal PDE inhibitor; milrinone, 3 µM, PDE3 inhibitor; rolipram, 3 µM, PDE4 inhibitor; sildenafil, 3 µM, PDE5 inhibitor; papaverine, 25 µM, PDE10 inhibitor) were applied respectively for 24 h. [^{3}H]-thymidine incorporation was performed in the last 4 h of stimulation. †††P < 0.001 *vs* 0.1% FBS, ***P < 0.001 *vs* 10% FBS. n = 4 in each group. Values are expressed as mean ± SEM.

4.9 Papaverine treatment on MCT-induced pulmonary hypertension in rats

4.9.1 Effect of papaverine on hemodynamics

Animal experiments with a MCT-induced PH rat model were performed to examine the therapeutic efficacy and anti-remodeling potential of PDE10A inhibition. Saline treated MCT-PH rats exhibited a significant increase in right ventricular systolic pressure (RVSP) on day 35 (77.2±9.74 *vs* 29.1±1.3 mm Hg) (Figure 22A), and in pulmonary vascular resistance index (PVRI) (2.90±0.24 *vs* 0.90±0.13 mm Hg min/ml 100 g body weight) (Figure 22C) as compared to control rats. No significant changes in systemic arterial pressure (SAP) and systemic vascular resistance index (SVRI) occurred (Figure 22B and 22D). Treatment of these rats by continuous infusion of papaverine from day 21 to day 35 resulted in a significant reduction of RVSP (48.4±5.3 mm Hg) (Figure 22A) and PVRI (1.73±0.28 mm Hg min/ml 100 g body weight) (Figure 22C), whereas SAP and SVRI did not change significantly (Figure 22B and 22D) as compared to saline treated animals.

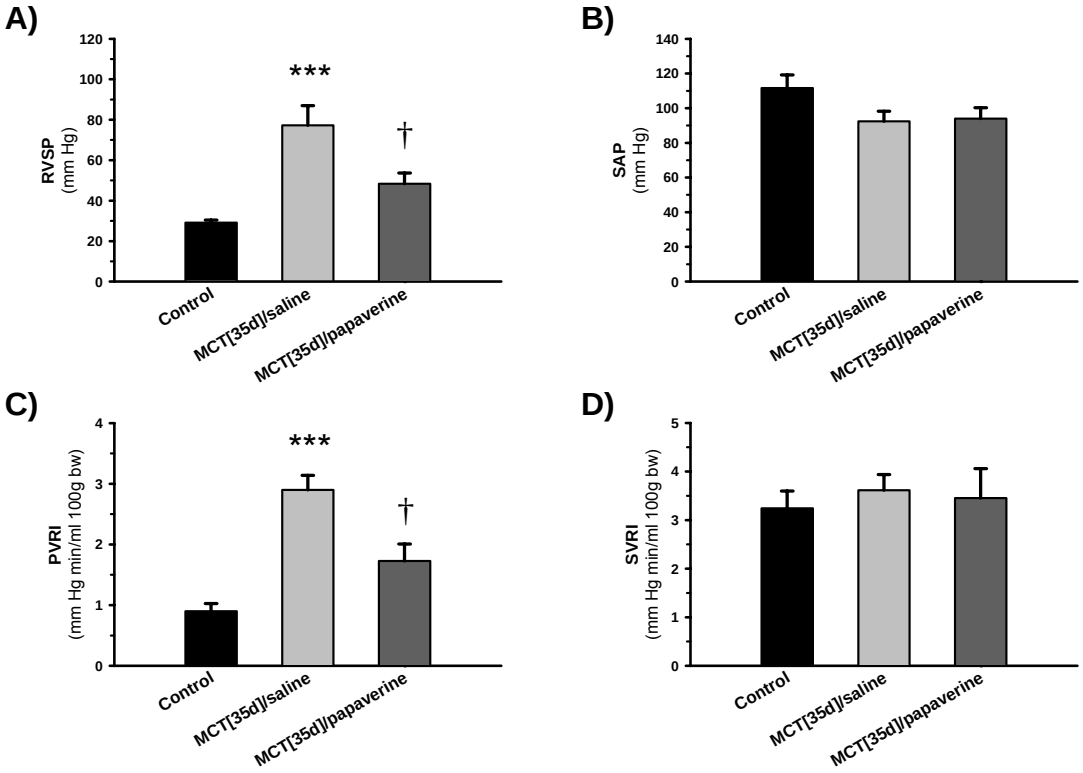

Figure 22: Effect of papaverine on hemodynamics of MCT-PH rats. Papaverine was applied by continuous intravenous infusion with osmotic minipumps from day 21 to day 35. Control: n=9; MCT[35d]/saline: n=8; MCT[35d]/papaverine: n=8. **A)** Right ventricular systolic pressure (RVSP, mmHg), **B)** systemic arterial pressure (SAP, mmHg), **C)** pulmonary vascular resistance index (PVRI, mmHg min/ml 100 g body) and **D)** systemic vascular resistance index (SVRI, mmHg) are given as mean ± SEM. ***P < 0.001 *vs* control; †P < 0.05 *vs* MCT[35d].

4.9.2 Effect of papaverine on pulmonary peripheral artery muscularization

Morphology analysis of the degree of muscularization of the peripheral small pulmonary arteries (Figure 23) showed that control rat lungs consisted of a majority of nonmuscularized arteries (79.5±4.5%), with a small percentage of partially muscularized arteries (14.0±4.0%) and a smaller percentage of fully muscularized arteries (6.5±0.5%). In contrast, the percentage of non-muscularized arteries decreased to 1.2±0.4%, and the percentage of partially and nonmuscularized arteries increased to 33.3±4.3% and 65.4±4.5% respectively, in saline treated MCT-PH rat lungs. Papaverine treatment decreased the proportion of fully muscularized arteries to 24.4±3.4%, accompanied by a significant increase in partially muscularized arteries to 70.5±2.7% and in nonmuscularized pulmonary arteries to 5.0±1.2% (Figure 23).

A)

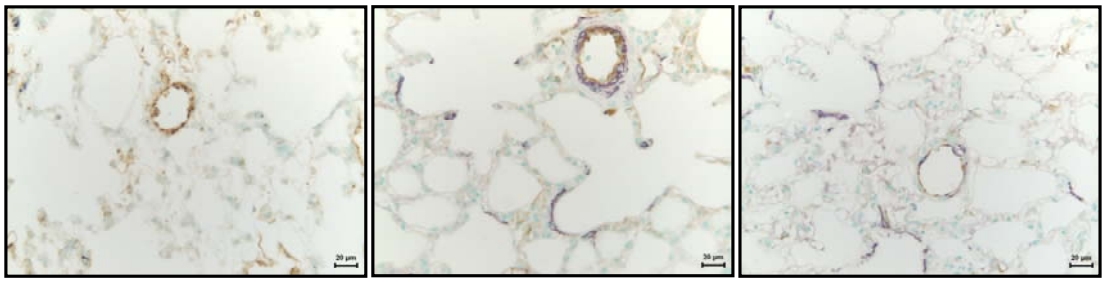

B)

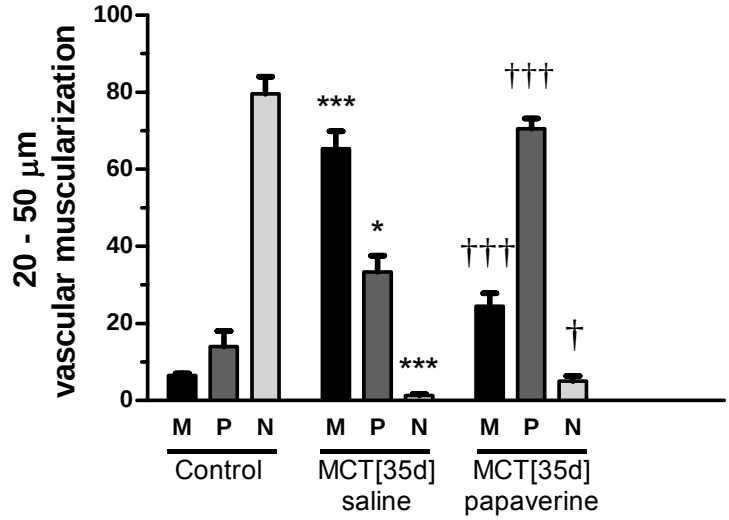

Figure 23: Effect of papaverine on the extent of muscularization of peripheral pulmonary arteries. A total of 80 to 100 intra-acinar vessels were analyzed in each lung from each group. **A)** Representative double immunostaining microphotographs of the rat lung sections to assess the muscularization of small pulmonary arteries. Staining was undertaken for von Willebrand-factor (brown, endothelial cells) and αSMA (purple, smooth muscle cells). **B)** The percentage of nonmuscularized (N), partially muscularized (P), or fully muscularized (M) pulmonary arteries related to the total number of pulmonary arteries is given as mean ± SEM. ***P < 0.001 *vs* control; †P < 0.05 *vs* MCT[35d].

4.10 PDE10A expression in human lungs from donors and IPAH patients

To ascertain clinical relevance of these findings, the expression and localization of PDE10A was investigated in human IPAH lungs by immunohistochemistry. As seen in Figure 8, a strong immunoreactivity of PDE10A was observed in pulmonary arteries, predominantly in the medial layer, of IPAH lung tissue (Figure 24, e-h). In contrast, only weak expression of PDE10A was detected in pulmonary arteries of donor lung tissue (Figure 24, a-d).

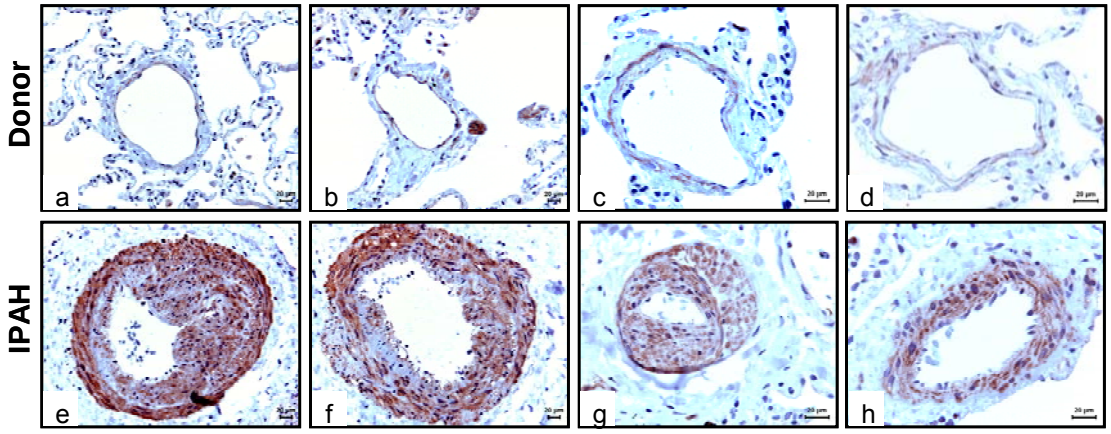

Figure 24: Pulmonary vascular expression and localization of PDE10A in lung tissues from donor and IPAH patients. Representative PDE10A immunostaining microphotographs of the human lung sections from donors (a-d) and IPAH patients (e-h). Scale bar: 20 µm.

5 DISCUSSION

It is widely accepted that phosphodiesterases are key factors regulating the pulmonary vascular tone[89-92] by mediating NO/cGMP pathway in pulmonary vasculature and PDE inhibitors are proved to be potent pulmonary artery relaxants in PAH[80, 93-95]. More recently, it was demonstrated that other than involvement in vascular tone, PDEs play an important role in modulating various signaling pathways in pulmonary vascular remodeling, via the tight control of the second messages - cAMP and cGMP. PDE1, PDE3, PDE4 and PDE5 have been reported to be increased in the vasculature of lung and inhibitors to those PDE subfamilies could suppress pulmonary vascular remodeling[78, 80-83, 96, 97]. However in addition to those well explored isoforms, there are some newly identified PDE isoforms (PDE7-11) in the PDE family. This brings up an important issue whether these PDEs are also involved in the pathogenesis of PAH. So it is of interest to determine the expression profile of those newly identified PDEs and to uncover which pathophysiological roles they may play in the development of PAH.

5.1 PDE7-11 in PAH

The present data demonstrate that multiple newly identified PDEs are expressed and altered (PDE7A, PDE7B and PDE10A) in the lungs of MCT-induced pulmonary hypertensive rats. The mRNA expression analysis of PDE7-11 in the lungs and in PASMCs demonstrated interesting tissue and cell specific patterns along with modulation of PDEs in healthy and hypertensive lungs. PDE10 isoform is mostly reported in brain diseases, based on the concept that PDE10A is not widely expressed outside of the central nervous system. However, we observed increased expression of PDE10A in MCT-PH lungs and MCT PASMCs as compared to controls. PDE7 is mostly involved in the immune system, such as T cell activation[98]. An upregulation of PDE7A and PDE7B was observed in MCT-PH rat lungs, whereas only PDE7A was upregulated in MCT-PH PASMCs as compared to control PASMCs, suggesting a distinct cellular localization of these two PDE7 isoforms. In accordance, PDE7A isoform was detected by RT-PCR in vascular SMCs other than in T lymphocytes, monocytes, neutrophils, airway SMCs, lung fibroblasts, epithelial

cells, and cardiac myocytes[99-102] and has been implicated in the pathogenesis of chronic obstructive pulmonary disease and asthma[100, 103]. However, protein expression analysis of PDE7A in lungs and in PASMCs revealed a weak expression of PDE7A in pulmonary vasculature and with no significant changes in MCT PASMCs as compared to control PASMCs (data not shown). This suggests discordance between transcriptional and translational regulation of PDE7A in MCT-induced pulmonary vascular remodeling and needs further investigations.

5.2 PDE10A in PAH

An immunohistochemical study of PDE10A localization in the major mammalian tissues demonstrated the lack of PDE10A immunoreactivity in the peripheral organs (liver, kidney, lung, spleen, or heart) of any species. Different from their finding, in our studies we found the presence of PDE10A in lung vasculature. Moreover, PDE10A expression is prominently induced in the structurally remodeled pulmonary arterial muscular layer. In accordance, PDE10A mRNA and protein expression are increased in PASMCs isolated from MCT-PH rats as compared to control rats. Moreover, PDE10A is one of the major cAMP hydrolyzing PDEs and contributes more to the total cAMP PDE activity in MCT-PH PASMCs compared with control PASMCs. Taken together, all these data suggest a likely contribution of PDE10A in the pathogenesis of PAH.

The tissue distribution and cellular localization of PDEs are important clues to understand their pathophysiological functions and apply potential therapeutic strategies. PDE expression in a particular organ or cell type could suggest potential effects of a corresponding PDE inhibitor *in vivo*. For example, high levels of PDE5 expression in corpus cavernosum and lung are consistent with the therapeutic benefits in treating erectile dysfunction and pulmonary hypertension, respectively[104, 105]. PDE10A was identified only 10 years ago and demands a better understanding of its functions. Unique distribution of PDE10A in the brain and its enrichment in the striatum, made PDE10A as a potential therapeutic target for the treatment of neurological and psychiatric disorders[106-109]. Recently nuclear PDE10A staining was noted in some endocrine organ and

PDE10A-selective inhibitors have also been claimed to be useful for the treatment of diabetes and obesity[110].

Although well characterized in brain, PDE10A is sparsely addressed in adult lung tissue[69]. The stronger expression in pulmonary arteries and in isolated PASMCs from the MCT-PH rat in our studies suggests that PDE10A may contribute to the proliferative phenotype of PASMCs. Although the specific functional role of PDE10A in lung tissue needs to be further characterized, this study also suggests a reactivation of PDE10A signaling in abnormal proliferative lung disease tissues, such as the tissues observed in pathological vascular remodeling. Moreover, we also found that PDE10A immunoreactivity was strongly increased in pulmonary arteries of IPAH patient lung sections as compared to the donors, indicating clinical relevance of the findings obtained from the MCT model.

5.3 Influence of PDE10A on PASMC proliferation

Vascular remodeling, which includes proliferation and hypertrophy of smooth muscle cells, is a characteristic feature of PAH[8, 111]. Recent studies have reported that targeting abnormal media proliferation blocks the development of PAH and attenuates pulmonary arterial remodeling in rodents and humans[8, 58, 59, 112]. In the MCT-induced PH model, we found that PASMCs from MCT rats are much more proliferative than PASMCs from control rats, a result consistent with the reports demonstrating that PASMCs from pulmonary hypertensive vessels possess larger mitogenic potent[85, 113]. In our studies, a selective PDE10A inhibitor as well as selective PDE10A siRNA suppressed proliferation of PASMCs. More interestingly, among the major cAMP-hydrolyzing PDE inhibitors, PDE10 inhibitor papaverine was the most potential one to reduce PASMC proliferation. In this aspect, PDE10 selective inhibitors may thus act as more efficient anti-proliferative drugs compared with other PDE specific inhibitors, implying that PDE10A could be a useful therapeutic target for PAH and for other disorders characterized by increased PASMC proliferation.

5.4 Signaling pathway related to anti-prolifeative effect of PDE10 inhibiton

Regarding to the critical role of cyclic nucleotide on cell proliferation, both cGMP and cAMP are believed to inhibit SMC proliferation *in vitro* and *in vivo*[114, 115]. By applying the 8-Br-cAMP, a cAMP analogue resistant to PDE-mediated hydrolysis, cell cycle traverse was suppressed[116]. Also the unspecific PDE inhibitor IBMX - by inhibiting cAMP hydrolysis - can block the PASMCs proliferation stimulated by growth factors[97]. Moreover PDE3 and PDE4, as cAMP- PDEs, have been shown to play an essential role in cAMP catabolism in experimental PAH models and combined PDE 3/4 inhibitors increase cAMP levels and reverse pulmonary vascular remodeling[82]. Although PDE10A is a dual-substrate PDE, it is reported that the enzyme activity is stimulated by cAMP being bind to the GAF domains of PDE10A[73, 74]. Taken together, we speculate that PDE10A may mainly control cAMP level under the pathophysiological conditions, although we can not exclude the involvement of cGMP[117].

These anti-proliferative effects are largely due to an increase in intracellular cAMP level that may subsequently stimulate the activity of protein kinase A (PKA)[118, 119]. cAMP, produced by activation of G protein-coupled receptors (GPCRs) and activation of adenylate cyclases, binds to the regulatory subunits of PKA to release the catalytic subunits. In the cytoplasm, PKA catalytic subunits phosphorylate downstream targets; while in the nucleus, PKA catalytic subunits phosphorylate cAMP response element-binding protein (CREB), resulting in activation of DNA transcription of cAMP-responsive element-containing genes. Deactivation of cAMP/PKA pathway is accomplished through degradation of cAMP to 5'AMP by cAMP-PDEs[120, 121] (Figure 25). In line with this notion, several studies from our group and others have reported that compounds which activate adenylate cyclase or inhibit PDE counteract several pathways involved in SMC proliferation[78, 83, 122]. For example, cAMP in vascular SMCs was shown to decrease the expression of cyclin D1 and cdk2 as well as extracellular signal-regulated kinase (ERK) activation, and to increase the expression of the anti-proliferative molecules such as p53 and p21[114, 123-125]. In addition, there is now substantial evidence that cAMP/PKA signaling acts as a molecular gate to block cell cycle progression, largely via occupancy of the

cAMP response elements (CRE) in the promoter region of the cyclin A gene, along with an increase in the level and phosphorylation status of the CREB transcription factor[126]. But intracellular mechanisms leading to CREB phosphorylation are diverse, as well as the cellular responses after CREB phosphorylation are multiple[127]. From the research of PDE10A in brain, it was demonstrated that papaverine increases cAMP level and CREB phosphorylation by inhibiting PDE10A[128]. In accordance, we found that the ratio of phosphorylated CREB to total CREB was significantly increased in PASMCs after PDE10A inhibition by papaverine and PDE10A-selective siRNA. This may have important consequences for PAH *in vivo*, since CREB content has been shown to be diminished in SMCs in remodeled pulmonary arteries with PAH[129].

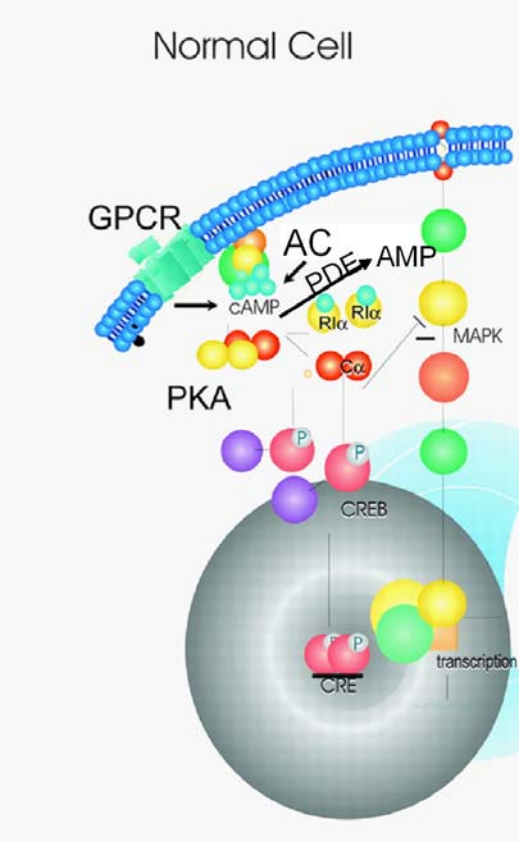

Figure 25: Diagram of the cAMP/PKA signaling in normal cells. (Modified from Bossis, I., 2004)

5.5 Therapeutic effects of a PDE10 inhibitor on MCT-induced PH

A couple of experimental or preclinical experiments showed PDE inhibitors exhibit therapeutic improvement not only via vascular relaxation, more

important, via reversing pulmonary vascular remodeling[78-81]. Cyclic nucleotide-mediated cellular responses are governed not only by alterations in PDE expression but also by the activity of specific types of PDE isoforms. Studies on hypoxic PAH rat suggests that decrease in intracellular cyclic nucleotide levels in pulmonary arteries from pulmonary hypertensive rats is associated with increased PDE activity[77, 113]. Recently, Murray et al., demonstrated that the total cAMP-PDE and cGMP-PDE activity is increased in PAH PASMCs as compared to control PASMCs[97]. They investigated only the contribution of PDE1-5 to the total cAMP PDE activity and concluded that the increased the cAMP activity is mainly from PDE3 isoform. In agreement with these findings, an increase in the total cAMP-PDE activity was observed in a well-established experimental model of PH in our study. Notably, the relative contribution of PDE10A to total cAMP-PDE activity was found to be increased in MCT-PH PASMCs as compared to control PASMCs, indicating that PDE10A inhibition was more effective in increasing cAMP generation and inhibiting hyperproliferation of PASMCs from MCT-PH rats. This suggests that PDE inhibitors that raise cAMP in general, as well as PDE10A-selective inhibitors, offer a new target for therapeutic intervention in pulmonary hypertension. In line, treatment of MCT-PH rats with the PDE10A inhibitor papaverine for 14 days markedly improved pulmonary hemodynamics. Right ventricular systolic pressure was significantly lowered as well as total pulmonary vascular resistance index with papaverine treatment, with no systemic effects. The structural changes of the lung vasculature such as high percentage of fully muscularized peripheral pulmonary arteries were significantly decreased with papaverine treatment. However, since papaverine is used as a potent vasodilator in the systemic and cerebral vasculature, we couldn't rule out the possibility that papaverine may exert vasodilatory effect on pulmonary vessels[130]. Papaverine-induced vasorelaxation is believed to be related to reduced calcium influx following PAK activation after cAMP increase[131, 132]. Of note, although papaverine offers a good opportunity for the preclinical studies as a relatively selective PDE10 inhibitor, still new PDE10 inhibitors with higher selectivity and potency are required to further explore the therapeutic aspects.

5.6 Limitations

A limitation of this study is that the *in vivo* experiments were carried out in MCT-induced PH rat model[133-135]. Monocrotaline is a toxic pyrrolizidine alkaloid from the plant Crotalaria spectablis. After a sinle injection of subcutaneous injection of MCT in rats, MCT is transformed in the liver to the active compound - MCT pyrrole, which bio-functionally leads to vascular injury[136]. Although it is the most commonly employed PH animal model to study the pathophysiological and possible therapeutic approaches, the exact mechanism through which MCT causes PH is not known completely yet. Most of the investigators believe that MCT causes endothelial injury, which eventually leads to medial hypertrophy and vasoconstriction in the pulmonary arterioles with no formation of intimal lesions in the peripheral pulmonary arteries[136, 137]. In contrast, the characteristic pathological changes in human pulmonary arterial hypertension include medial hypertrophy, intimal proliferation, in situ thrombosis, and plexiform lesions[138]. Thus, the results obtained from the MCT model may not be predictive of response to therapy in humans and needs to be evaluated in other alternative animal models of PAH. However, the increased immunoreactivity of PDE10A in remodelled pulmonary vasculature of IPAH patients show clinical relevance and promise to proceed further.

5.7 Conclusion and perspectives

In the present study, PDE10A expression and activity are shown to be increased in lung tissue and PASMCs of experimental PH. Loss-of-function studies using the PDE10A inhibitor papaverine and PDE10A-targeted siRNA showed increased cAMP generation and CREB phosphorylation, and reduced proliferation of PASMCs from MCT-PH rats. However the mechanism underlying those effects has not been clearly demonstrated. The common cAMP/PKA signaling is shown in the schematic overview of Figure 26. Agonists such as prostacyclin bind to receptors and activate G proteins, which in turn activate adenylyl cyclase to release cAMP. After binding of cAMP to the homodimer of regulatory subunits (RIα), catalytic subunits (PKA^C) are released. Cytoplasma PKA^C phosphorylates multiple cytoplasmatic targets. PKA^C can also been translocated to nucleus and phosphorylates CREB, resulting in activation of DNA transcription of CRE-containing gene. We found that PDE10A

is majorly presented in nucleus, so it would be important to investigate if this specific compartmentalization of PDE10A regulates degradation of nuclear cAMP and cGMP, which may mediate relative cellular responses contributing to vascular remodeling.

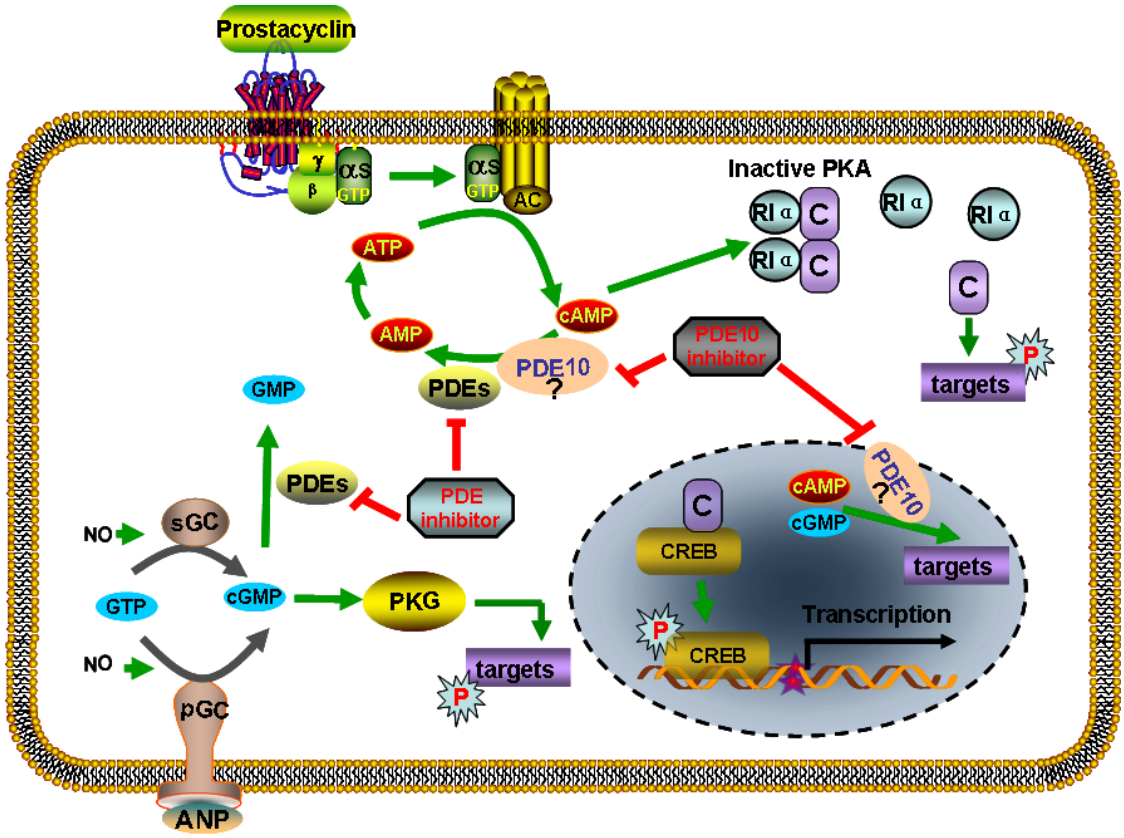

Figure 26: Scheme of cyclic nucleotide signaling system regulated by PDE10 in PASMCs.

The cellular response demonstrated that PDE10A plays a major role in the hyperproliferation of PASMCs. Furthermore, intravenous infusion of papaverine significantly improved pulmonary hemodynamics and significantly reversed structural changes underlying MCT-induced PH in rats. To the best of our knowledge this is the first study indicating a central role of PDE10A in progressive pulmonary vascular remodelling. Based on our findings, we speculate that PDE10 inhibition present a novel therapeutic approach to the treatment of PAH.

Taken together, we have shown in this study the role of PDE10A in pulmonary vascular remodeling in a MCT-PH rat model and this offers another potent

theorapeutic option for PAH. It is of interest to examine on other models such as hypoxia PH model, as well to evaluate that if PDE10A is importantly involved in the pathogenesis of PAH patients.

6 REFERENCES

(1) Rubin LJ. Primary pulmonary hypertension. *N Engl J Med* 1997 January 9;336(2):111-7.

(2) Romberg E. 1891. Ueber slerose der lungenarterien. *Deutsch Arch Klin Med*. 48, 197.

(3) DRESDALE DT, SCHULTZ M, MICHTOM RJ. Primary pulmonary hypertension. I. Clinical and hemodynamic study. *Am J Med* 1951 December;11(6):686-705.

(4) Gaine SP, Rubin LJ. Primary pulmonary hypertension. *Lancet* 1998 August 29;352(9129):719-25.

(5) Simonneau G, Galie N, Rubin LJ, Langleben D, Seeger W, Domenighetti G, Gibbs S, Lebrec D, Speich R, Beghetti M, Rich S, Fishman A. Clinical classification of pulmonary hypertension. *J Am Coll Cardiol* 2004 June 16;43(12 Suppl S):5S-12S.

(6) Simonneau G, Robbins IM, Beghetti M, Channick RN, Delcroix M, Denton CP, Elliott CG, Gaine SP, Gladwin MT, Jing ZC, Krowka MJ, Langleben D, Nakanishi N, Souza R. Updated clinical classification of pulmonary hypertension. *J Am Coll Cardiol* 2009 June 30;54(1 Suppl):S43-S54.

(7) Rabinovitch M. Molecular pathogenesis of pulmonary arterial hypertension. *J Clin Invest* 2008 July;118(7):2372-9.

(8) Stenmark KR, Mecham RP. Cellular and molecular mechanisms of pulmonary vascular remodeling. *Annu Rev Physiol* 1997;59:89-144.

(9) Farber HW, Loscalzo J. Pulmonary arterial hypertension. *N Engl J Med* 2004 October 14;351(16):1655-65.

(10) Johnson SR, Granton JT, Mehta S. Thrombotic arteriopathy and anticoagulation in pulmonary hypertension. *Chest* 2006 August;130(2):545-52.

(11) Humbert M, Morrell NW, Archer SL, Stenmark KR, MacLean MR, Lang IM, Christman BW, Weir EK, Eickelberg O, Voelkel NF, Rabinovitch M. Cellular and molecular pathobiology of pulmonary arterial hypertension. *J Am Coll Cardiol* 2004 June 16;43(12 Suppl S):13S-24S.

(12) Archer S, Rich S. Primary pulmonary hypertension: a vascular biology and translational research "Work in progress". *Circulation* 2000 November 28;102(22):2781-91.

(13) Chan SY, Loscalzo J. Pathogenic mechanisms of pulmonary arterial hypertension. *J Mol Cell Cardiol* 2008 January;44(1):14-30.

(14) Giaid A, Saleh D. Reduced expression of endothelial nitric oxide synthase in the lungs of patients with pulmonary hypertension. *N Engl J Med* 1995 July 27;333(4):214-21.

(15) Fagan KA, Fouty BW, Tyler RC, Morris KG, Jr., Hepler LK, Sato K, LeCras TD, Abman SH, Weinberger HD, Huang PL, McMurtry IF, Rodman DM. The pulmonary circulation of homozygous or heterozygous eNOS-null mice is hyperresponsive to mild hypoxia. *J Clin Invest* 1999 January;103(2):291-9.

(16) Champion HC, Bivalacqua TJ, Greenberg SS, Giles TD, Hyman AL, Kadowitz PJ. Adenoviral gene transfer of endothelial nitric-oxide synthase (eNOS) partially restores normal pulmonary arterial pressure in eNOS-deficient mice. *Proc Natl Acad Sci U S A* 2002 October 1;99(20):13248-53.

(17) Zuckerbraun BS, Stoyanovsky DA, Sengupta R, Shapiro RA, Ozanich BA, Rao J, Barbato JE, Tzeng E. Nitric oxide-induced inhibition of smooth muscle cell proliferation involves S-nitrosation and inactivation of RhoA. *Am J Physiol Cell Physiol* 2007 February;292(2):C824-C831.

(18) Radomski MW, Palmer RM, Moncada S. An L-arginine/nitric oxide pathway present in human platelets regulates aggregation. *Proc Natl Acad Sci U S A* 1990 July;87(13):5193-7.

(19) Gerber JG, Voelkel N, Nies AS, McMurtry IF, Reeves JT. Moderation of hypoxic vasoconstriction by infused arachidonic acid: role of PGI2. *J Appl Physiol* 1980 July;49(1):107-12.

(20) Christman BW, McPherson CD, Newman JH, King GA, Bernard GR, Groves BM, Loyd JE. An imbalance between the excretion of thromboxane and prostacyclin metabolites in pulmonary hypertension. *N Engl J Med* 1992 July 9;327(2):70-5.

(21) Tuder RM, Cool CD, Geraci MW, Wang J, Abman SH, Wright L, Badesch D, Voelkel NF. Prostacyclin synthase expression is decreased in lungs from patients with severe pulmonary hypertension. *Am J Respir Crit Care Med* 1999 June;159(6):1925-32.

(22) Petkov V, Mosgoeller W, Ziesche R, Raderer M, Stiebellehner L, Vonbank K, Funk GC, Hamilton G, Novotny C, Burian B, Block LH. Vasoactive intestinal peptide as a new drug for treatment of primary pulmonary hypertension. *J Clin Invest* 2003 May;111(9):1339-46.

(23) Hamidi SA, Prabhakar S, Said SI. Enhancement of pulmonary vascular remodelling and inflammatory genes with VIP gene deletion. *Eur Respir J* 2008 January;31(1):135-9.

(24) Said SI, Hamidi SA, Dickman KG, Szema AM, Lyubsky S, Lin RZ, Jiang YP, Chen JJ, Waschek JA, Kort S. Moderate pulmonary arterial hypertension in male mice lacking the vasoactive intestinal peptide gene. *Circulation* 2007 March 13;115(10):1260-8.

(25) Li H, Chen SJ, Chen YF, Meng QC, Durand J, Oparil S, Elton TS. Enhanced endothelin-1 and endothelin receptor gene expression in chronic hypoxia. *J Appl Physiol* 1994 September;77(3):1451-9.

(26) Giaid A, Yanagisawa M, Langleben D, Michel RP, Levy R, Shennib H, Kimura S, Masaki T, Duguid WP, Stewart DJ. Expression of endothelin-1 in the lungs of patients with pulmonary hypertension. *N Engl J Med* 1993 June 17;328(24):1732-9.

(27) Seo B, Oemar BS, Siebenmann R, von SL, Luscher TF. Both ETA and ETB receptors mediate contraction to endothelin-1 in human blood vessels. *Circulation* 1994 March;89(3):1203-8.

(28) Pollock DM, Keith TL, Highsmith RF. Endothelin receptors and calcium signaling. *FASEB J* 1995 September;9(12):1196-204.

(29) Ohlstein EH, Arleth A, Bryan H, Elliott JD, Sung CP. The selective endothelin ETA receptor antagonist BQ123 antagonizes endothelin-1-mediated mitogenesis. *Eur J Pharmacol* 1992 April 10;225(4):347-50.

(30) Hirata Y, Emori T, Eguchi S, Kanno K, Imai T, Ohta K, Marumo F. Endothelin receptor subtype B mediates synthesis of nitric oxide by cultured bovine endothelial cells. *J Clin Invest* 1993 April;91(4):1367-73.

(31) Dupuis J, Goresky CA, Fournier A. Pulmonary clearance of circulating endothelin-1 in dogs in vivo: exclusive role of ETB receptors. *J Appl Physiol* 1996 October;81(4):1510-5.

(32) Yuan XJ, Wang J, Juhaszova M, Gaine SP, Rubin LJ. Attenuated K+ channel gene transcription in primary pulmonary hypertension. *Lancet* 1998 March 7;351(9104):726-7.

(33) Michelakis ED, McMurtry MS, Wu XC, Dyck JR, Moudgil R, Hopkins TA, Lopaschuk GD, Puttagunta L, Waite R, Archer SL. Dichloroacetate, a metabolic

modulator, prevents and reverses chronic hypoxic pulmonary hypertension in rats: role of increased expression and activity of voltage-gated potassium channels. *Circulation* 2002 January 15;105(2):244-50.

(34) MacLean MR, Sweeney G, Baird M, McCulloch KM, Houslay M, Morecroft I. 5-Hydroxytryptamine receptors mediating vasoconstriction in pulmonary arteries from control and pulmonary hypertensive rats. *Br J Pharmacol* 1996 November;119(5):917-30.

(35) Lee SL, Wang WW, Lanzillo JJ, Fanburg BL. Serotonin produces both hyperplasia and hypertrophy of bovine pulmonary artery smooth muscle cells in culture. *Am J Physiol* 1994 January;266(1 Pt 1):L46-L52.

(36) MacLean MR, Herve P, Eddahibi S, Adnot S. 5-hydroxytryptamine and the pulmonary circulation: receptors, transporters and relevance to pulmonary arterial hypertension. *Br J Pharmacol* 2000 September;131(2):161-8.

(37) Launay JM, Herve P, Peoc'h K, Tournois C, Callebert J, Nebigil CG, Etienne N, Drouet L, Humbert M, Simonneau G, Maroteaux L. Function of the serotonin 5-hydroxytryptamine 2B receptor in pulmonary hypertension. *Nat Med* 2002 October;8(10):1129-35.

(38) Marcos E, Adnot S, Pham MH, Nosjean A, Raffestin B, Hamon M, Eddahibi S. Serotonin transporter inhibitors protect against hypoxic pulmonary hypertension. *Am J Respir Crit Care Med* 2003 August 15;168(4):487-93.

(39) Guignabert C, Izikki M, Tu LI, Li Z, Zadigue P, Barlier-Mur AM, Hanoun N, Rodman D, Hamon M, Adnot S, Eddahibi S. Transgenic mice overexpressing the 5-hydroxytryptamine transporter gene in smooth muscle develop pulmonary hypertension. *Circ Res* 2006 May 26;98(10):1323-30.

(40) Olschewski H, Rose F, Schermuly R, Ghofrani HA, Enke B, Olschewski A, Seeger W. Prostacyclin and its analogues in the treatment of pulmonary hypertension. *Pharmacol Ther* 2004 May;102(2):139-53.

(41) Higenbottam T, Wheeldon D, Wells F, Wallwork J. Long-term treatment of primary pulmonary hypertension with continuous intravenous epoprostenol (prostacyclin). *Lancet* 1984 May 12;1(8385):1046-7.

(42) Rubin LJ, Mendoza J, Hood M, McGoon M, Barst R, Williams WB, Diehl JH, Crow J, Long W. Treatment of primary pulmonary hypertension with continuous intravenous prostacyclin (epoprostenol). Results of a randomized trial. *Ann Intern Med* 1990 April 1;112(7):485-91.

(43) Olschewski H, Walmrath D, Schermuly R, Ghofrani A, Grimminger F, Seeger W. Aerosolized prostacyclin and iloprost in severe pulmonary hypertension. *Ann Intern Med* 1996 May 1;124(9):820-4.

(44) Hoeper MM, Schwarze M, Ehlerding S, dler-Schuermeyer A, Spiekerkoetter E, Niedermeyer J, Hamm M, Fabel H. Long-term treatment of primary pulmonary hypertension with aerosolized iloprost, a prostacyclin analogue. *N Engl J Med* 2000 June 22;342(25):1866-70.

(45) Hoeper MM, Spiekerkoetter E, Westerkamp V, Gatzke R, Fabel H. Intravenous iloprost for treatment failure of aerosolised iloprost in pulmonary arterial hypertension. *Eur Respir J* 2002 August;20(2):339-43.

(46) Simonneau G, Barst RJ, Galie N, Naeije R, Rich S, Bourge RC, Keogh A, Oudiz R, Frost A, Blackburn SD, Crow JW, Rubin LJ. Continuous subcutaneous infusion of treprostinil, a prostacyclin analogue, in patients with pulmonary arterial hypertension: a double-blind, randomized, placebo-controlled trial. *Am J Respir Crit Care Med* 2002 March 15;165(6):800-4.

(47) Pepke-Zaba J, Higenbottam TW, nh-Xuan AT, Stone D, Wallwork J. Inhaled nitric oxide as a cause of selective pulmonary vasodilatation in pulmonary hypertension. *Lancet* 1991 November 9;338(8776):1173-4.

(48) Evgenov OV, Pacher P, Schmidt PM, Hasko G, Schmidt HH, Stasch JP. NO-independent stimulators and activators of soluble guanylate cyclase: discovery and therapeutic potential. *Nat Rev Drug Discov* 2006 September;5(9):755-68.

(49) Evgenov OV, Kohane DS, Bloch KD, Stasch JP, Volpato GP, Bellas E, Evgenov NV, Buys ES, Gnoth MJ, Graveline AR, Liu R, Hess DR, Langer R, Zapol WM. Inhaled agonists of soluble guanylate cyclase induce selective pulmonary vasodilation. *Am J Respir Crit Care Med* 2007 December 1;176(11):1138-45.

(50) Dumitrascu R, Weissmann N, Ghofrani HA, Dony E, Beuerlein K, Schmidt H, Stasch JP, Gnoth MJ, Seeger W, Grimminger F, Schermuly RT. Activation of soluble guanylate cyclase reverses experimental pulmonary hypertension and vascular remodeling. *Circulation* 2006 January 17;113(2):286-95.

(51) Grimminger F, Weimann G, Frey R, Voswinckel R, Thamm M, Bolkow D, Weissmann N, Muck W, Unger S, Wensing G, Schermuly RT, Ghofrani HA. First acute haemodynamic study of soluble guanylate cyclase stimulator riociguat in pulmonary hypertension. *Eur Respir J* 2009 January 7.

(52) Rubin LJ, Badesch DB, Barst RJ, Galie N, Black CM, Keogh A, Pulido T, Frost A, Roux S, Leconte I, Landzberg M, Simonneau G. Bosentan therapy for pulmonary arterial hypertension. *N Engl J Med* 2002 March 21;346(12):896-903.

(53) McLaughlin VV, Sitbon O, Badesch DB, Barst RJ, Black C, Galie N, Rainisio M, Simonneau G, Rubin LJ. Survival with first-line bosentan in patients with primary pulmonary hypertension. *Eur Respir J* 2005 February;25(2):244-9.

(54) Barst RJ, Langleben D, Badesch D, Frost A, Lawrence EC, Shapiro S, Naeije R, Galie N. Treatment of pulmonary arterial hypertension with the selective endothelin-A receptor antagonist sitaxsentan. *J Am Coll Cardiol* 2006 May 16;47(10):2049-56.

(55) Galie N, Olschewski H, Oudiz RJ, Torres F, Frost A, Ghofrani HA, Badesch DB, McGoon MD, McLaughlin VV, Roecker EB, Gerber MJ, Dufton C, Wiens BL, Rubin LJ. Ambrisentan for the treatment of pulmonary arterial hypertension: results of the ambrisentan in pulmonary arterial hypertension, randomized, double-blind, placebo-controlled, multicenter, efficacy (ARIES) study 1 and 2. *Circulation* 2008 June 10;117(23):3010-9.

(56) Michelakis E, Tymchak W, Lien D, Webster L, Hashimoto K, Archer S. Oral sildenafil is an effective and specific pulmonary vasodilator in patients with pulmonary arterial hypertension: comparison with inhaled nitric oxide. *Circulation* 2002 May 21;105(20):2398-403.

(57) Galie N, Ghofrani HA, Torbicki A, Barst RJ, Rubin LJ, Badesch D, Fleming T, Parpia T, Burgess G, Branzi A, Grimminger F, Kurzyna M, Simonneau G. Sildenafil citrate therapy for pulmonary arterial hypertension. *N Engl J Med* 2005 November 17;353(20):2148-57.

(58) Schermuly RT, Dony E, Ghofrani HA, Pullamsetti S, Savai R, Roth M, Sydykov A, Lai YJ, Weissmann N, Seeger W, Grimminger F. Reversal of experimental pulmonary hypertension by PDGF inhibition. *J Clin Invest* 2005 October;115(10):2811-21.

(59) Ghofrani HA, Seeger W, Grimminger F. Imatinib for the treatment of pulmonary arterial hypertension. *N Engl J Med* 2005 September 29;353(13):1412-3.

(60) Patterson KC, Weissmann A, Ahmadi T, Farber HW. Imatinib mesylate in the treatment of refractory idiopathic pulmonary arterial hypertension. *Ann Intern Med* 2006 July 18;145(2):152-3.

(61) Souza R, Sitbon O, Parent F, Simonneau G, Humbert M. Long term imatinib treatment in pulmonary arterial hypertension. *Thorax* 2006 August;61(8):736.

(62) SHMAN DF, LIPTON R, MELICOW MM, PRICE TD. Isolation of adenosine 3', 5'-monophosphate and guanosine 3', 5'-monophosphate from rat urine. *Biochem Biophys Res Commun* 1963 May 22;11:330-4.

(63) Conti M, Beavo J. Biochemistry and physiology of cyclic nucleotide phosphodiesterases: essential components in cyclic nucleotide signaling. *Annu Rev Biochem* 2007;76:481-511.

(64) Matsumoto T, Kobayashi T, Kamata K. Phosphodiesterases in the vascular system. *J Smooth Muscle Res* 2003 August;39(4):67-86.

(65) Beavo JA. Cyclic nucleotide phosphodiesterases: functional implications of multiple isoforms. *Physiol Rev* 1995 October;75(4):725-48.

(66) Lugnier C. Cyclic nucleotide phosphodiesterase (PDE) superfamily: a new target for the development of specific therapeutic agents. *Pharmacol Ther* 2006 March;109(3):366-98.

(67) Soderling SH, Beavo JA. Regulation of cAMP and cGMP signaling: new phosphodiesterases and new functions. *Curr Opin Cell Biol* 2000 April;12(2):174-9.

(68) Bender AT, Beavo JA. Cyclic nucleotide phosphodiesterases: molecular regulation to clinical use. *Pharmacol Rev* 2006 September;58(3):488-520.

(69) Fujishige K, Kotera J, Michibata H, Yuasa K, Takebayashi S, Okumura K, Omori K. Cloning and characterization of a novel human phosphodiesterase that hydrolyzes both cAMP and cGMP (PDE10A). *J Biol Chem* 1999 June 25;274(26):18438-45.

(70) Soderling SH, Bayuga SJ, Beavo JA. Isolation and characterization of a dual-substrate phosphodiesterase gene family: PDE10A. *Proc Natl Acad Sci U S A* 1999 June 8;96(12):7071-6.

(71) Loughney K, Snyder PB, Uher L, Rosman GJ, Ferguson K, Florio VA. Isolation and characterization of PDE10A, a novel human 3', 5'-cyclic nucleotide phosphodiesterase. *Gene* 1999 June 24;234(1):109-17.

(72) Fujishige K, Kotera J, Omori K. Striatum- and testis-specific phosphodiesterase PDE10A isolation and characterization of a rat PDE10A. *Eur J Biochem* 1999 December;266(3):1118-27.

(73) Handa N, Mizohata E, Kishishita S, Toyama M, Morita S, Uchikubo-Kamo T, Akasaka R, Omori K, Kotera J, Terada T, Shirouzu M, Yokoyama S. Crystal structure of the GAF-B domain from human phosphodiesterase 10A complexed with its ligand, cAMP. *J Biol Chem* 2008 July 11;283(28):19657-64.

(74) Gross-Langenhoff M, Hofbauer K, Weber J, Schultz A, Schultz JE. cAMP is a ligand for the tandem GAF domain of human phosphodiesterase 10 and cGMP for the tandem GAF domain of phosphodiesterase 11. *J Biol Chem* 2006 February 3;281(5):2841-6.

(75) Chappie TA, Humphrey JM, Allen MP, Estep KG, Fox CB, Lebel LA, Liras S, Marr ES, Menniti FS, Pandit J, Schmidt CJ, Tu M, Williams RD, Yang FV. Discovery of a series of 6,7-dimethoxy-4-pyrrolidylquinazoline PDE10A inhibitors. *J Med Chem* 2007 January 25;50(2):182-5.

(76) Theo SR, Ardeschir GH, Weissmann N. Prostanoids and phosphodiesterase inhibitors in experimental pulmonary hypertension. *Curr Top Dev Biol* 2005;67:251-84.

(77) Maclean MR, Johnston ED, Mcculloch KM, Pooley L, Houslay MD, Sweeney G. Phosphodiesterase isoforms in the pulmonary arterial circulation of the rat: changes in pulmonary hypertension. *J Pharmacol Exp Ther* 1997 November;283(2):619-24.

(78) Schermuly RT, Pullamsetti SS, Kwapiszewska G, Dumitrascu R, Tian X, Weissmann N, Ghofrani HA, Kaulen C, Dunkern T, Schudt C, Voswinckel R, Zhou J, Samidurai A, Klepetko W, Paddenberg R, Kummer W, Seeger W, Grimminger F. Phosphodiesterase 1 upregulation in pulmonary arterial hypertension: target for reverse-remodeling therapy. *Circulation* 2007 May 1;115(17):2331-9.

(79) Murray F, MacLean MR, Pyne NJ. Increased expression of the cGMP-inhibited cAMP-specific (PDE3) and cGMP binding cGMP-specific (PDE5) phosphodiesterases in models of pulmonary hypertension. *Br J Pharmacol* 2002 December;137(8):1187-94.

(80) Schermuly RT, Kreisselmeier KP, Ghofrani HA, Yilmaz H, Butrous G, Ermert L, Ermert M, Weissmann N, Rose F, Guenther A, Walmrath D, Seeger W, Grimminger F. Chronic sildenafil treatment inhibits monocrotaline-induced pulmonary hypertension in rats. *Am J Respir Crit Care Med* 2004 January 1;169(1):39-45.

(81) Wharton J, Strange JW, Moller GM, Growcott EJ, Ren X, Franklyn AP, Phillips SC, Wilkins MR. Antiproliferative effects of phosphodiesterase type 5 inhibition in human pulmonary artery cells. *Am J Respir Crit Care Med* 2005 July 1;172(1):105-13.

(82) Pullamsetti S, Krick S, Yilmaz H, Ghofrani HA, Schudt C, Weissmann N, Fuchs B, Seeger W, Grimminger F, Schermuly RT. Inhaled tolafentrine reverses pulmonary vascular remodeling via inhibition of smooth muscle cell migration. *Respir Res* 2005;6:128.

(83) Phillips PG, Long L, Wilkins MR, Morrell NW. cAMP phosphodiesterase inhibitors potentiate effects of prostacyclin analogs in hypoxic pulmonary vascular remodeling. *Am J Physiol Lung Cell Mol Physiol* 2005 January;288(1):L103-L115.

(84) Schermuly RT, Kreisselmeier KP, Ghofrani HA, Samidurai A, Pullamsetti S, Weissmann N, Schudt C, Ermert L, Seeger W, Grimminger F. Antiremodeling effects of iloprost and the dual-selective phosphodiesterase 3/4 inhibitor tolafentrine in chronic experimental pulmonary hypertension. *Circ Res* 2004 April 30;94(8):1101-8.

(85) Lai YJ, Pullamsetti SS, Dony E, Weissmann N, Butrous G, Banat GA, Ghofrani HA, Seeger W, Grimminger F, Schermuly RT. Role of the prostanoid EP4 receptor in iloprost-mediated vasodilatation in pulmonary hypertension. *Am J Respir Crit Care Med* 2008 July 15;178(2):188-96.

(86) Thompson WJ, Appleman MM. Characterization of cyclic nucleotide phosphodiesterases of rat tissues. *J Biol Chem* 1971 May 25;246(10):3145-50.

(87) Bauer AC, Schwabe U. An improved assay of cyclic 3',5'-nucleotide phosphodiesterases with QAE-Sephadex columns. *Naunyn Schmiedebergs Arch Pharmacol* 1980 March;311(2):193-8.

(88) Zurbonsen K, Michel A, Vittet D, Bonnet PA, Chevillard C. Dissociation between phosphodiesterase inhibition and antiproliferative effects of phosphodiesterase inhibitors on the Dami cell line. *Biochem Pharmacol* 1997 April 25;53(8):1141-7.

(89) Pauvert O, Salvail D, Rousseau E, Lugnier C, Marthan R, Savineau JP. Characterisation of cyclic nucleotide phosphodiesterase isoforms in the media layer of the main pulmonary artery. *Biochem Pharmacol* 2002 May 1;63(9):1763-72.

(90) Pauvert O, Bonnet S, Rousseau E, Marthan R, Savineau JP. Sildenafil alters calcium signaling and vascular tone in pulmonary arteries from chronically

hypoxic rats. *Am J Physiol Lung Cell Mol Physiol* 2004 September;287(3):L577-L583.

(91) Clarke WR, Uezono S, Chambers A, Doepfner P. The type III phosphodiesterase inhibitor milrinone and type V PDE inhibitor dipyridamole individually and synergistically reduce elevated pulmonary vascular resistance. *Pulm Pharmacol* 1994 April;7(2):81-9.

(92) Sweeney G, Templeton A, Clayton RA, Baird M, Sheridan S, Johnston ED, MacLean MR. Contractile responses to sumatriptan in isolated bovine pulmonary artery rings: relationship to tone and cyclic nucleotide levels. *J Cardiovasc Pharmacol* 1995 November;26(5):751-60.

(93) Rabe KF, Tenor H, Dent G, Schudt C, Nakashima M, Magnussen H. Identification of PDE isozymes in human pulmonary artery and effect of selective PDE inhibitors. *Am J Physiol* 1994 May;266(5 Pt 1):L536-L543.

(94) Jeffery TK, Wanstall JC. Phosphodiesterase III and V inhibitors on pulmonary artery from pulmonary hypertensive rats: differences between early and established pulmonary hypertension. *J Cardiovasc Pharmacol* 1998 August;32(2):213-9.

(95) Cohen AH, Hanson K, Morris K, Fouty B, McMurty IF, Clarke W, Rodman DM. Inhibition of cyclic 3'-5'-guanosine monophosphate-specific phosphodiesterase selectively vasodilates the pulmonary circulation in chronically hypoxic rats. *J Clin Invest* 1996 January 1;97(1):172-9.

(96) Dony E, Lai YJ, Dumitrascu R, Pullamsetti SS, Savai R, Ghofrani HA, Weissmann N, Schudt C, Flockerzi D, Seeger W, Grimminger F, Schermuly RT. Partial reversal of experimental pulmonary hypertension by phosphodiesterase-3/4 inhibition. *Eur Respir J* 2008 March;31(3):599-610.

(97) Murray F, Patel HH, Suda RY, Zhang S, Thistlethwaite PA, Yuan JX, Insel PA. Expression and activity of cAMP phosphodiesterase isoforms in pulmonary artery smooth muscle cells from patients with pulmonary hypertension: role for PDE1. *Am J Physiol Lung Cell Mol Physiol* 2007 January;292(1):L294-L303.

(98) Li L, Yee C, Beavo JA. CD3- and CD28-dependent induction of PDE7 required for T cell activation. *Science* 1999 February 5;283(5403):848-51.

(99) Guo J, Watson A, Kempson J, Carlsen M, Barbosa J, Stebbins K, Lee D, Dodd J, Nadler SG, McKinnon M, Barrish J, Pitts WJ. Identification of potent pyrimidine

inhibitors of phosphodiesterase 7 (PDE7) and their ability to inhibit T cell proliferation. *Bioorg Med Chem Lett* 2009 April 1;19(7):1935-8.

(100) Smith SJ, Brookes-Fazakerley S, Donnelly LE, Barnes PJ, Barnette MS, Giembycz MA. Ubiquitous expression of phosphodiesterase 7A in human proinflammatory and immune cells. *Am J Physiol Lung Cell Mol Physiol* 2003 February;284(2):L279-L289.

(101) Michaeli T, Bloom TJ, Martins T, Loughney K, Ferguson K, Riggs M, Rodgers L, Beavo JA, Wigler M. Isolation and characterization of a previously undetected human cAMP phosphodiesterase by complementation of cAMP phosphodiesterase-deficient Saccharomyces cerevisiae. *J Biol Chem* 1993 June 15;268(17):12925-32.

(102) Fuhrmann M, Jahn HU, Seybold J, Neurohr C, Barnes PJ, Hippenstiel S, Kraemer HJ, Suttorp N. Identification and function of cyclic nucleotide phosphodiesterase isoenzymes in airway epithelial cells. *Am J Respir Cell Mol Biol* 1999 February;20(2):292-302.

(103) Jones NA, Leport M, Holand T, Vos T, Morgan M, Fink M, Pruniaux MP, Berthelier C, O'Connor BJ, Bertrand C, Page CP. Phosphodiesterase (PDE) 7 in inflammatory cells from patients with asthma and COPD. *Pulm Pharmacol Ther* 2007;20(1):60-8.

(104) Gopal VK, Francis SH, Corbin JD. Allosteric sites of phosphodiesterase-5 (PDE5). A potential role in negative feedback regulation of cGMP signaling in corpus cavernosum. *Eur J Biochem* 2001 June;268(11):3304-12.

(105) Corbin JD, Beasley A, Blount MA, Francis SH. High lung PDE5: a strong basis for treating pulmonary hypertension with PDE5 inhibitors. *Biochem Biophys Res Commun* 2005 September 2;334(3):930-8.

(106) Xie Z, Adamowicz WO, Eldred WD, Jakowski AB, Kleiman RJ, Morton DG, Stephenson DT, Strick CA, Williams RD, Menniti FS. Cellular and subcellular localization of PDE10A, a striatum-enriched phosphodiesterase. *Neuroscience* 2006 May 12;139(2):597-607.

(107) Siuciak JA, Chapin DS, Harms JF, Lebel LA, McCarthy SA, Chambers L, Shrikhande A, Wong S, Menniti FS, Schmidt CJ. Inhibition of the striatum-enriched phosphodiesterase PDE10A: a novel approach to the treatment of psychosis. *Neuropharmacology* 2006 August;51(2):386-96.

(108) Hebb AL, Robertson HA. Role of phosphodiesterases in neurological and psychiatric disease. *Curr Opin Pharmacol* 2007 February;7(1):86-92.

(109) Menniti FS, Chappie TA, Humphrey JM, Schmidt CJ. Phosphodiesterase 10A inhibitors: a novel approach to the treatment of the symptoms of schizophrenia. *Curr Opin Investig Drugs* 2007 January;8(1):54-9.

(110) Cantin LD, Magnuson S, Gunn D, Barucci N, Breuhaus M, Bullock WH, Burke J, Claus TH, Daly M, Decarr L, Gore-Willse A, Hoover-Litty H, Kumarasinghe ES, Li Y, Liang SX, Livingston JN, Lowinger T, Macdougall M, Ogutu HO, Olague A, Ott-Morgan R, Schoenleber RW, Tersteegen A, Wickens P, Zhang Z, Zhu J, Zhu L, Sweet LJ. PDE-10A inhibitors as insulin secretagogues. *Bioorg Med Chem Lett* 2007 May 15;17(10):2869-73.

(111) Mandegar M, Fung YC, Huang W, Remillard CV, Rubin LJ, Yuan JX. Cellular and molecular mechanisms of pulmonary vascular remodeling: role in the development of pulmonary hypertension. *Microvasc Res* 2004 September;68(2):75-103.

(112) Merklinger SL, Jones PL, Martinez EC, Rabinovitch M. Epidermal growth factor receptor blockade mediates smooth muscle cell apoptosis and improves survival in rats with pulmonary hypertension. *Circulation* 2005 July 19;112(3):423-31.

(113) Kunichika N, Landsberg JW, Yu Y, Kunichika H, Thistlethwaite PA, Rubin LJ, Yuan JX. Bosentan inhibits transient receptor potential channel expression in pulmonary vascular myocytes. *Am J Respir Crit Care Med* 2004 November 15;170(10):1101-7.

(114) Bornfeldt KE, Krebs EG. Crosstalk between protein kinase A and growth factor receptor signaling pathways in arterial smooth muscle. *Cell Signal* 1999 July;11(7):465-77.

(115) Rybalkin SD, Yan C, Bornfeldt KE, Beavo JA. Cyclic GMP phosphodiesterases and regulation of smooth muscle function. *Circ Res* 2003 August 22;93(4):280-91.

(116) Southgate K, Newby AC. Serum-induced proliferation of rabbit aortic smooth muscle cells from the contractile state is inhibited by 8-Br-cAMP but not 8-Br-cGMP. *Atherosclerosis* 1990 May;82(1-2):113-23.

(117) Sano H, Nagai Y, Miyakawa T, Shigemoto R, Yokoi M. Increased social interaction in mice deficient of the striatal medium spiny neuron-specific phosphodiesterase 10A2. *J Neurochem* 2008 April;105(2):546-56.

(118) Iyengar R. Gating by cyclic AMP: expanded role for an old signaling pathway. *Science* 1996 January 26;271(5248):461-3.

(119) Koyama H, Bornfeldt KE, Fukumoto S, Nishizawa Y. Molecular pathways of cyclic nucleotide-induced inhibition of arterial smooth muscle cell proliferation. *J Cell Physiol* 2001 January;186(1):1-10.

(120) Bossis I, Stratakis CA. Minireview: PRKAR1A: normal and abnormal functions. *Endocrinology* 2004 December;145(12):5452-8.

(121) Dwivedi Y, Pandey GN. Adenylyl cyclase-cyclicAMP signaling in mood disorders: Role of the crucial phosphorylating enzyme protein kinase A. *Neuropsychiatr Dis Treat* 2008 February;4(1):161-76.

(122) Rybalkin SD, Bornfeldt KE, Sonnenburg WK, Rybalkina IG, Kwak KS, Hanson K, Krebs EG, Beavo JA. Calmodulin-stimulated cyclic nucleotide phosphodiesterase (PDE1C) is induced in human arterial smooth muscle cells of the synthetic, proliferative phenotype. *J Clin Invest* 1997 November 15;100(10):2611-21.

(123) Vadiveloo PK, Filonzi EL, Stanton HR, Hamilton JA. G1 phase arrest of human smooth muscle cells by heparin, IL-4 and cAMP is linked to repression of cyclin D1 and cdk2. *Atherosclerosis* 1997 August;133(1):61-9.

(124) Graves LM, Bornfeldt KE, Raines EW, Potts BC, Macdonald SG, Ross R, Krebs EG. Protein kinase A antagonizes platelet-derived growth factor-induced signaling by mitogen-activated protein kinase in human arterial smooth muscle cells. *Proc Natl Acad Sci U S A* 1993 November 1;90(21):10300-4.

(125) Hayashi S, Morishita R, Matsushita H, Nakagami H, Taniyama Y, Nakamura T, Aoki M, Yamamoto K, Higaki J, Ogihara T. Cyclic AMP inhibited proliferation of human aortic vascular smooth muscle cells, accompanied by induction of p53 and p21. *Hypertension* 2000 January;35(1 Pt 2):237-43.

(126) Kothapalli D, Stewart SA, Smyth EM, Azonobi I, Pure E, Assoian RK. Prostacylin receptor activation inhibits proliferation of aortic smooth muscle cells by regulating cAMP response element-binding protein- and pocket protein-dependent cyclin a gene expression. *Mol Pharmacol* 2003 August;64(2):249-58.

(127) Shaywitz AJ, Greenberg ME. CREB: a stimulus-induced transcription factor activated by a diverse array of extracellular signals. *Annu Rev Biochem* 1999;68:821-61.

(128) Rajadhyaksha A, Leveque J, Macias W, Barczak A, Konradi C. Molecular components of striatal plasticity: the various routes of cyclic AMP pathways. *Dev Neurosci* 1998;20(2-3):204-15.

(129) Klemm DJ, Watson PA, Frid MG, Dempsey EC, Schaack J, Colton LA, Nesterova A, Stenmark KR, Reusch JE. cAMP response element-binding protein content is a molecular determinant of smooth muscle cell proliferation and migration. *J Biol Chem* 2001 December 7;276(49):46132-41.

(130) Christensen CW, Rosen LB, Gal RA, Haseeb M, Lassar TA, Port SC. Coronary vasodilator reserve. Comparison of the effects of papaverine and adenosine on coronary flow, ventricular function, and myocardial metabolism. *Circulation* 1991 January;83(1):294-303.

(131) Aoki H, Nishimura J, Kobayashi S, Kanaide H. Relationship between cytosolic calcium concentration and force in the papaverine-induced relaxation of medial strips of pig coronary artery. *Br J Pharmacol* 1994 February;111(2):489-96.

(132) Torres-Flores V, Hernandez-Rueda YL, Neri-Vidaurri PC, Jimenez-Trejo F, Calderon-Salinas V, Molina-Guarneros JA, Gonzalez-Martinez MT. Activation of protein kinase A stimulates the progesterone-induced calcium influx in human sperm exposed to the phosphodiesterase inhibitor papaverine. *J Androl* 2008 September;29(5):549-57.

(133) Heath D. The rat is a poor animal model for the study of human pulmonary hypertension. *Cardioscience* 1992 March;3(1):1-6.

(134) Robbins IM. Advancing therapy for pulmonary arterial hypertension: can animal models help? *Am J Respir Crit Care Med* 2004 January 1;169(1):5-6.

(135) Stenmark KR, Meyrick B, Galie N, Mooi WJ, McMurtry IF. ANIMAL MODELS OF PULMONARY ARTERIAL HYPERTENSION The Hope for Etiologic Discovery and Pharmacologic Cure. *Am J Physiol Lung Cell Mol Physiol* 2009 September 11.

(136) Chesney CF, Allen JR. Animal model: pulmonary hypertension, cor pulmonale and endocardial fibroelastosis in monocrotaline-intoxicated nonhuman primates. *Am J Pathol* 1973 March;70(3):489-92.

(137) Schultze AE, Roth RA. Chronic pulmonary hypertension--the monocrotaline model and involvement of the hemostatic system. *J Toxicol Environ Health B Crit Rev* 1998 October;1(4):271-346.

(138) Zaiman A, Fijalkowska I, Hassoun PM, Tuder RM. One hundred years of research in the pathogenesis of pulmonary hypertension. *Am J Respir Cell Mol Biol* 2005 November;33(5):425-31.

7 ERKLÄRUNG

Ich erkläre: Ich habe die vorgelegte Dissertation selbständig, ohne unerlaubte fremde Hilfe und nur mit den Hilfen angefertigt, die ich in der Dissertaion angegeben habe. Alle Textstellen, die wörtlich oder sinngemäß aus veröffentlichten oder nicht veröffentlichten Schriften entnommen sind, und alle Angaben, die auf mündlichen Auskünften beruhen, sind als solche kenntlich gemacht. Bei den von mir durchgeführten und in der Dissertation erwähnten Untersuchungen habe ich die Grundsätze guter wissenschaftlicher Praxis, wie sie in der Satzung der Justus-Liebig-Universität Gießen zur Sicherung guter wissenschaftlicher Praxis niedergelegt sind, eingehalten.

Giessen, Dec. 2009 **Xia Tian**

8 ACKNOWLEDGEMENTS

My deepest gratitude goes first and foremost to my supervisor, Prof. Dr. Ralph Schermuly. His professional guidance, constant encouragement and support kept me all the way on track during my scientific research.

Also I would express heartfelt gratitude to Prof. Dr. Werner Seeger, who motivates me entering pulmonary research and provides all possible conditions for research.

I sincerely thank Prof. Dr. Oliver Eickelberg and Dr. Rory Morty for their excellent tutoring in the MBML (Molecular Biology and Medicine of the Lung) graduate program.

I own great gratitude to Dr. Soni Savai Pullamsetti, not only for her initiation of this project, her intellectual suggestions and helpful comments, but also for her precious care and friendship. It gave me great pleasure to work with her.

I would like to thank all my wonderful colleagues for teaching me techniques, offering experimental tips and more important for the nice working atmosphere they have created. To be more specific, I would like to express gratitude to Dr. Yingju-Lai for sharing her experience on cell culture and sister-friendly support in work as well as in life; to Dr. Kathrin Woyda for her precise instructions on work and strong nerves for translating a lot of documents including the German version of summary here in the thesis; to Dr. Raj Savai for his instructive suggestions; to Christina Vroom for her big efforts on animal experiments; to Ewa Bieniek for the help with immunohistochemistry; to Dr. Ewa Kolosionek, Dr. Sevdalina Nikolova, Dr. Sergey B. Udalov, Piotr Sklepkiewicz, Aleksandra Tretyn, Joachim Berk, Lal Kurian and Mattias Eschenhagen for all the helps and friendship; to Caroline Zoerb, Susanne Ficus, Matthias Hecker and Katharina Weidl for their technical assistant; also to other colleagues, too numerous to mention, who helped in their own little way throughout this work. “Thank you very much”.

My thanks also extend to Prof. Dr. Friedrich Grimminger, Dr. Ardeschir Ghofrani and Dr. Norbert Weissmann for the cooperative support.

I would like to take this opportunity to thank Deutsche Forschungsgemeinschaft and Nycomed Konstanz for the financial support.

Further I highly appreciate my Chinese friends for their kind help and moral support during my study.

Last but not least, I am especially indebted to my beloved parents for everything they have done for me all through these years. Without the love and encourage from them, I can never have the chance to finish my study.